Patrícia Alexandra Leido Batista

Studying Genetic Damage and Repair using 3D Breast Cancer Cell Models

ORIENTADORAS

Maria Helena Caria, Professora Doutora, IPS/ESS

Susana Nunes da Silva, Professora Doutora, NMS/UNL, Comprehensive Health Research Centre (CHRC)

December 2025

Presidente: Professor Célio Gabriel Figueiredo Pina, ESTSetúbal/IPS

Orientador: Professora Susana Maria Nunes da Silva Duarte Catana, NMS/UNL

Arguente: Professor Francisco Vaz De Carvalho Esteves, ESS/IPS

Acknowledgements

First of all, I would like to thank my orienteers, professors Helena Caria and Susana Nunes Silva, for the guidance and support throughout this research journey. I also want to show my gratitude to Polytechnic Institute of Setúbal and Nova Medical School, for providing the opportunity to carry out this study. In particular, I would like to thank the Comprehensive Health Research Centre (CHRC), thank you for the availability and all the resources provided, including laboratory access and technical assistance, as well as the supportive research environment that significantly contributed for my learning experience.

I am deeply grateful to my family, partner and friends. You were the ones who kept me going through all the chaos, stress and were very patient and supportive during this process. To my mom, dad, sister and brother-in-law, thank you for believing in me and for providing the reassurance I needed during the most challenging moments.

To my partner, Henrique, thank you for your incredible patience and understanding, for being there through every up and down, and for never letting me give up. All your support truly made all the difference.

To my best friend and course colleague, Raquel, I can't thank you enough for the last six years we've shared, you were always there for the good and the bad, for every laugh and every cry. Thanks to you, I was never alone in this difficult journey, and for that, I am forever grateful. To my dear friends, Miguel and Maria, I appreciate your care, patience and constant motivation, it would never have been the same without you.

Lastly, I want to express my gratitude to all my laboratory colleagues. More importantly, to Laura and Diogo, thank you for sharing your knowledge and for being the greatest guides I could have asked for. And thank you to Catarina, Jhenifer and Mariana, for always being available for me when I needed it, you kept me going through it all.

Resumo

O cancro da mama continua a ser uma das principais causas de morte entre mulheres em todo o mundo. O objetivo desde estudo foi avaliar os efeitos do peróxido de hidrogénio (H_2O_2) e da doxorrubicina (DOX) em três linhas celulares mamárias – MCF-10A (controlo), MCF-7 e MDA-MB-231 – cultivadas em duas e três dimensões (esferóides). A lesão no DNA foi avaliado através do ensaio Cometa e foi também realizada uma análise morfológica. Ambos os agentes induziram lesão significativa no DNA, com maior sensibilidade observada nas culturas 2D. Os esferóides apresentaram maior resistência, destacando a importância da dimensionalidade na resposta a fármacos e ao stress oxidativo na investigação do cancro da mama.

Palavras-passe: Cancro da mama, Peróxido de Hidrogénio, Doxorrubicina, Esferóides, Dano no DNA, Ensaio Cometa

Abstract

Breast cancer (BC) remains one of the leading causes of death among women worldwide. The aim of this study was to evaluate the effects of hydrogen peroxide (H_2O_2) and doxorubicin (DOX) in three BC cell lines – MCF-10A (control), MCF-7 and MDA-MB-231 – both in two-dimensional (2D) and three-dimensional (3D) cultures (spheroids). DNA damage was assessed using the Comet Assay and a morphological analysis was also performed. Both agents induced significant DNA damage, with higher sensitivity observed in 2D cultures. The 3D spheroids presented increased resistance, highlighting the importance of dimensionality, in both drug response and oxidative stress in BC research.

Key-words: Breast cancer, Hydrogen Peroxide, Doxorubicin, Spheroids, DNA damage, Comet Assay

Index

Figure Index

Table Index

List of Abbreviations and Acronyms

2D: Two-dimensional

3D: Three-dimensional

AP: Apurinic/Apyrimidinic

ATM: Ataxia-telangiectasia mutated

BC: Breast Cancer

BCT: Breast Conserving Therapy

BER: Base Excision Repair

BRCA1: Breast Cancer gene 1

BRCA2: Breast Cancer gene 2

Check 2: Checkpoint Kinase 2

CO_2: Carbon Dioxide

CTx: Choleric Toxin

CT: Computed Tomography

CZI: Carl Zeiss Image

DDR: DNA Damage Response

ddH_2O: Double-distilled water

dH_2O: Distilled water

DMEM: Dulbecco's Modified Eagles Medium

DMEM-F12: Dulbecco's Modified Eagles Medium – Nutrient Mixture F12

DMEM-HG: Dulbecco's Modified Eagles Medium – High Glucose

DMEM-LG: Dulbecco's Modified Eagles Medium – Low Glucose

DMSO: Dimethyl Sulfoxide

DOX: Doxorubicin

DSBs: Double-Strand Breaks

ECG: Electrocardiogram

ECM: Extracellular Matrix

EDTA: Ethylenediaminetetraacetic Acid

EGF: Epidermal Growth Factor

ER+: Estrogen Receptor positive

FBS: Fetal Bovine Serum

FDA: Food and Drug Administration

G1: Gap 1 phase

G2: Gap 2 phase

GG-NER: Global Genome - Nucleotide Excision Repair

H_2O_2: Hydrogen Peroxide

HER-: Human Epidermal Growth Factor negative

HER2+: Human Epidermal Growth Factor positive

HR: Homologous Repair

HS: Horse Serum

IR: Ionizing Radiation

LMP: Low Melting Point

MDR: Multidrug Resistance

MEM: Minimum Essential Medium

MMR: Mismatch Repair

MRI: Magnetic Resonance Imaging

NaCl: Sodium Chloride

NaOH: Sodium Hydroxide

NC: Negative Control

NER: Nucleotide Excision Repair

NHEJ: Non-homologous End Joining

p53: Tumour suppressor protein 53

PBS: Phosphate-Buffered Saline

Penstrep: Penicillin-Streptomycin

PR+: Progesterone positive

rBM: Reconstituted Basement Membrane

RONS: Reactive Oxygen and Nitrogen Species

ROS: Reactive Oxygen Species

rpm: Revolutions per minute

RT: Radiotherapy

S: Synthesis phase

SSBs: Single-Strand Breaks

TIFF: Tagged Image File Format

TM: Tail Moment

TNBC: Triple-negative Breast Cancer

TOP2A: Topoisomerase IIa

TC-NER: Transcription-Coupled - Nucleotide Excision Repair

UV: Ultraviolet

1. Introduction

This work focuses on the study of DNA damage, chemoresistance and drug effects induced on breast cancer (BC)-derived cell-lines, aiming to interconnect tri-dimensional (3D) models (spheroids) morphology, cancer subtypes and treatment responses in order to provide a deeper insight into breast cancer research.

As two-dimensional (2D) cell culture systems fail to accurately replicate tumours microenvironment, physiology as well as treatment responses and 3D models, such as spheroids, offer a more physiologically relevant alternative, which better mimics tumour architecture, cell-cell interactions and nutrient and oxygen gradients. Thus, this study was motivated by the need to address the gap between both models, by evaluating DNA damage, chemoresistance, treatments responses and spheroids morphology. Such insights may contribute to the development of more reliable preclinical models and support more personalized treatment strategies for BC patients.

The dissertation begins with an Introduction that contextualizes BC, detailing its epidemiology, risk factors, clinical staging, monitoring strategies and molecular subtypes, also reviewing current treatment approaches, emphasizing chemotherapy and doxorubicin. The second chapter focuses on DNA damage and repair, describing different types of DNA lesions, DNA damage responses and main repair pathways. The third chapter introduces cell culture models, comparing 2D and 3D systems, while also providing a characterization of the three cell-lines used on the study (MCF-7, MCF-10A, MDA-MB-231). Chapter four presents the Comet Assay, explaining its principle, methodology and limitations as a tool for assessing DNA damage at the single-cell level.

The next chapter refers to the methodology of the work, describing experimental procedures, including 2D and 3D cell culture conditions, treatment protocols, comet assay execution and data analysis. The Results and Discussion section integrates morphological characterization of spheroids with quantitative DNA damage analysis, comparing responses across cell-lines, treatments and the model's dimensionality, connecting spheroid morphology, chemoresistance and DNA damage, highlighting the importance of 3D models. Finally, this work ends with a conclusion summarizing the main findings and their implications on BC research, followed by references and annexes.

1.1. Breast Cancer

It is known worldwide that cancer is one of the most fatal diseases affecting humanity and the number of patients affected with this disease is continuously rising. Within the vast number of cancer types existing, women suffer mainly from BC, given the fact that about 1 in each 8 women will undergo this illness in their lifetime, causing it to be the most frequent cause of death – cancer related – among individuals of female gender, going over 520 000 deaths per year (Imamura et al., 2015; Lovitt et al., 2015; Nunes et al., 2019).

The commonly named Western lifestyle is one of the major causes for this pattern, being linked to a poor diet, smoking, high levels of stress and lack of physical activity, which are all key factors for cancer. Even though the exact cause of carcinogenesis remains unclear, the risk factors for breast cancer are well-known. The most significant ones include gender and age. Around 99% of breast cancer cases appear in women and only 1% affect men. However, the occurrence of breast cancer in men, much like in women, has been progressively rising, most likely linked to factors such as obesity and increased longevity. In terms of age, the worldwide rise is seen in all age groups, with a higher incidence in women under 50 years (Smolarz et al., 2022).

Hormonal issues are also of extreme importance, especially those related to the time of estrogen exposure and reproductive factors such as the number of children the woman has given birth to, the age at which a woman had the first child and breastfeeding. Having fewer children or not breastfeeding – or breastfeeding for a shorter period – can also contribute to a greater risk, as result of the higher number of menstrual cycles the woman will endure and, thus, a higher estrogen exposure (Smolarz et al., 2022; Wilkinson & Gathani, 2022). In particular, the appearance of menarche at a younger age than usual can be associated with an increased probability of having breast cancer, due to the prolonged exposure to estrogen over a longer period, which also happens at a more advanced age, when reaching menopause. Brinton et. al described that starting menstruation at age 15 or older is linked to a 23% lower risk of breast cancer compared to starting menstruation before age 12; nowadays, it is considered that this reduction in risk is around 30%. Additionally, it was found that an early start of menarche is linked to a higher probability of developing breast cancer when compared to a late menopause. For each additional year

of late menopause, the risk increases around 2,9%, which is lesser than the 5% of each year of early menarche (Smolarz et al., 2022).

Genetic predisposition is another key factor, even though less than 10% of breast cancer cases are known to be genetic – approximately 50% of the cases are linked to *BRCA1* or *BRCA2* gene mutations – and most of the tumours appear due to sporadic somatic mutations. The probability of having breast cancer for women with a mother or sister (first degree relatives) who have been treated for this kind of tumour is twice as high and increases for three to six times if the two closest family members have suffered from this disease. Population-based research has grouped numerous harmful gene mutations into high, moderate and low penetrance genes based on the associated risk of developing breast cancer. High penetrance genes, like *BRCA1* or *BRCA2,* lead to a breast cancer risk three times higher than the general population, while moderate penetrance genes – *CHEK2* (Checkpoint Kinase 2), increase the risk by 2 to 3 times and low penetrance genes – ATM (Ataxia-Telangiectasia Mutated) – contribute to a 1 to 2 times elevated risk (Smolarz et al., 2022, Hong & Xu, 2022).

Another significant risk factors include the use of hormonal contraception, alcohol consumption and exposure to ionizing radiation at a young age. The latter could damage the DNA and increase the production of reactive oxygen and nitrogen species (RONS), both directly and indirectly. RONS contribute to further DNA damage and may lead to mutations and genomic instability, caused by epigenetic changes. Therefore, their presence amplifies key factors that can lead to breast cancer as well as inflammation – result of the damage caused by RONS –, which not only intensifies the production of RONS and DNA lesions but also promotes the appearance of breast cancer by encouraging pro-carcinogenic effects on cells and tissues (Smolarz et al., 2022).

Even though the current 5-year survival rate due to breast cancer is 90%, there is still many deaths caused by the limited efficacy of the ongoing treatments. The failure of therapeutic and surgical procedures to eliminate all abnormal cells without promoting progression or inducing quiescence, metastasis and/or recurrence has been linked to drug resistance (Fisher & Rao, 2020). Cancer cells can develop this resistance at the very start of the treatment or after several drug administrations, becoming capable of deflecting the action of the drug, leading to lower efficacy in therapeutic treatments. This increase in cancer cells resistance may be the reason to why progression-free survival after second-line chemotherapy is lower than after first-line treatment (Nunes et al., 2019).

Breast cancer is classified into five different stages, going from 0 to IV, which help deciding the type of treatment needed for each patient. This classification is formed according to tumour size, lymph node involvement and the presence of metastasis, as shown in Table 1.1 (About breast cancer staging and grades, 2023).

Table 1.1 – Summary of BC stages and Characteristics *(*About Breast Cancer Staging and Grades*, 2023)*.

Stage	Description	Extent of Spread	Common Terminology
0	Ductal carcinoma in situ; pre-invasive cancer	Confined to breast ducts; does not spread to surrounding tissue	Pre-invasive / non-invasive breast cancer
I (IA–IB)	Small tumour; may involve nearby lymph nodes	Limited to breast or nearby nodes	Early stage breast cancer
II (IIA–IIB)	Larger tumour and/or greater lymph node involvement	Breast and nearby lymph nodes	Early stage breast cancer
III (IIIA–IIIC)	Spread to lymph nodes, thoracic wall or skin	Locally advanced; no distant metastasis	Locally advanced breast cancer
IV	Spread to distant organs	Distant metastasis	Advanced / metastatic breast cancer

1.1.1. Breast Cancer Monitoring

Breast cancer monitoring recommendations should be adapted based on a woman's risk level, which is divided in average risk or increased risk. The most used technique for diagnosing is the mammography, being acknowledged as the primary screening method and it is specifically effective for women from the age of 50 to 69 (Hong & Xu, 2022; Smolarz et al., 2022).

A mammography consists of an x-ray of the breast area, being able to reveal benign or malignant abnormalities, and can be applied to screening or diagnostic purposes; if for screening, mammograms aim to detect early signs of BC before any symptoms appear, with the goal of an early diagnosis; if it has diagnostic purposes, then they are used to investigate symptoms like a palpable lump in the breast (Bhushan et al., 2021). The fact that it uses ionizing radiation is considered a disadvantage, along with the low accuracy in younger women, giving many false-positive results due to their breast density. (Bhushan et al., 2021).

For women with known hereditary risk of breast cancer, an MRI has better use as a screening tool. This is a non-invasive modality that is very effective in accurately identifying and measuring tumours with 2 centimetres or less and detect any metastases

in women previously diagnosed with breast cancer. However, it may lead to unnecessary biopsies due to the incapability to differentiate between malignant and benign tumours (Bhushan et al., 2021).

1.1.2. Subtypes of Breast Cancer

Breast cancer is a heterogeneous disease, being divided into four main immunohistochemical sub-types where the differences between tumours are mainly due to its morphology or the receptor expression. The sub-types are based on their surface receptors, existing the estrogen receptor positive (ER+), the human epidermal growth factor positive (HER2+), the progesterone receptor positive (PR+) and the triple negative (TNBC) (Fisher & Rao, 2020; Lovitt et al., 2015; Orrantia-Borunda et al., 2022).

Generally, breast cancers are estrogen-dependent, developing when estrogen-sensitive tissues proliferate as a reaction to estrogens and suffer tumorigenesis. Roughly 70-75% of invasive breast cancers exhibit a notably high level of ER expression; therefore the estrogen receptor is a crucial diagnostic factor. More than half of ER+ patients also express the PR+, but it very unlikely for it to be expressed in those with ER- (estrogen receptor negative) breast cancer. As the progesterone receptor expression is controlled by the ER, the physiological PR values provide information regarding the functional ER pathway; nonetheless, both have high expression levels in breast cancer cells and are seen as diagnostic and prognostic biomarkers of breast cancer (Orrantia-Borunda et al., 2022; Smolarz et al., 2022).

The HER2 is mostly important for selecting appropriate treatment options, as its expression is found in 15–25% of breast cancers. Its overexpression is an early event in breast carcinogenesis and enhances the detection rate of both metastatic and recurrent breast cancer by 50-80% (Orrantia-Borunda et al., 2022).

Both HER2 and Ki67 (antigen used as a biomarker of cell proliferation) are crucial biomarkers in cancer biology, providing valuable insights in tumour aggressiveness, treatment response and prognosis. The Ki67 is a nuclear protein existent in all phases of the cell division process, apart from the resting phase of G0, and thus in every actively proliferating cell. This protein expression levels are essential for selecting adequate treatment strategies and planning follow-ups, with high Ki67 expression (more than 20%) correlating with lower survival rates (Smolarz et al., 2022). Similarly, the overexpression of the HER2 or its amplification hold significant prognostic and predictive value for

targeted treatments. The patient's prognosis may be highly improved if drugs that block the HER2 are applied, like trastuzumab (Orrantia-Borunda et al., 2022; Smolarz et al., 2022).

There are four major molecular subtypes of breast cancer, classified based on the gene's overexpression: luminal A, luminal B, HER2 positive and TNBC, as seen on Table 1.2.

Table 1.2- Characteristics of the four mentioned breast cancer subtypes. (p53 – tumour suppressor protein) ('Orrantia-Borunda et al., 2022)

	Luminal A	**Luminal B**	**HER2+**	**TNBC**
ER	Yes	Yes	Some cases	No
PR	Yes	Some cases	Some cases	No
HER2	No	No	Yes	No
Mutations	No	*BRCA2*	p53	*BRCA1* and p53
Progonosis	Good	Middle	Middle/Bad	Bad
Treatment	Hormonal	Hormonal/Chemotherapy	Hormonal/Chemotherapy	Chemotherapy

The first one is a low-grade breast cancer categorized by the presence of only ER and/or PR, presenting a low expression of protein Ki67. Luminal A is a slow growing type of cancer and has the best prognosis, corresponding to less incidence of relapse and higher survival rate, when compared to other types. The tumours display a high response rate to hormone therapy but worse results from chemotherapy. The tumours of luminal B breast cancer can show both ER and/or PR and present a high expression of Ki67 whether it is HER2- or HER2+. Luminal B breast cancers are of intermediate or high grade, due to the higher Ki67 levels, resulting in a more aggressive cancer that luminal A cancers, worsening its prognostic. Around 10-20% of all luminal carcinomas are of the luminal B type. They respond well to hormone therapy and benefit more from chemotherapy than the luminal A type of tumours (Bhushan et al., 2021; Orrantia-Borunda et al., 2022; Smolarz et al., 2022)

The HER2+ positive subtype constitutes from 10% to 15% of all breast cancers. The carcinomas are negative for both estrogen and progesterone receptors, while being positive for the HER2. These tumours have a higher proliferation rate that the ones of the luminal types, as well as high rate of metastasis. This is a more aggressive subtype, and it can be divided into two subgroups: the luminal HER2: ER+, PR+, HER2+ and Ki67: 15-30%; and HER2-enriched: ER-, PR-, HER2+ and Ki67>30%. The prognosis is worse when compared to luminal A and B tumours, but it has shown improvement when HER2-targeted drugs are applied, however, drug resistance or severe side effects may be a

limitation for clinical application of targeted therapy drugs. The treatment requires certain drugs against the HER2 protein, as extension to surgery or chemotherapy treatment – to which these types of tumours tend to have a higher response rate (Bhushan et al., 2021; Orrantia-Borunda et al., 2022; Smolarz et al., 2022).

The fourth subtype is the TNBC, where all the previous mentioned surface receptors are negative. Around 20% of all breast cancers are of this type and it is more frequent in women younger than 40 years old; women possessing *BRCA1* gene mutations also have higher probability to develop TNBC. This subtype is characterized by its aggressiveness, and the development of these tumours may vary with age, genetics, breastfeeding or weight. There is also a tendency for early relapses and to become noticeable in a more advanced stage. The TNBC has an elevated proliferation rate, genomic instability and provokes changes in the DNA repair genes. Under histological examination, it is a poorly differentiated, highly proliferative, and heterogenous tumour, consisting of subsets with differing prognoses (Bhushan et al., 2021; Orrantia-Borunda et al., 2022).

1.2. Treatment for Breast Cancer

Typically, cancer treatment relies on detecting tumour lesions using suitable diagnostic imaging techniques, followed by treatment through chemotherapy, radiotherapy or surgery. Precise diagnostics are of extreme importance for an early therapeutic intervention; if the diagnostic is not accurate, the treatments might be delayed, increasing the risk of death (Bhushan et al., 2021).

Radiotherapy (RT) remains a key component in the treatment of breast cancer, from early stages to more advanced or metastatic cases. Traditionally, RT for breast cancer consists of two-dimensional treatments over 5 to 7 weeks. However, modern techniques, like Computed Tomography (CT) have not only shortened the treatment time but also improved outcomes by reducing the risk of both immediate and long-term side effects while enhancing local control over the cancer growth, reducing exposure to nearby organs (Shah et al., 2024).

Surgical treatments include tumour removal, mastectomy (complete breast removal), excision of the sentinel lymph node or of the axillary lymph node. The mastectomy is performed in patients who, given the advanced stage of the disease, are considered unsuitable for a breast-conserving surgery or those who choose not to undergo breast-sparing procedures; it involves removing the entire breast along with the skin covering

the mammary gland. A breast conserving therapy (BCT) is usually applied in early stages of cancer, and its use is increasing as it is considered as effective as a mastectomy (Smolarz et al., 2022).

Chemotherapy is primarily used as a systemic adjuvant or neoadjuvant treatment to eliminate undetected micro-metastases, reduce recurrence and improve long-term survival outcomes (Hassan et al., 2010). The preferred procedure usually involves sequential use of taxane-based drugs, with or without anthracyclines (like Doxorrubicin - DOX), though its use may be considered in cases with a higher risk of recurrence. When deciding on adjuvant chemotherapy, factors such as tumour grade and size, growth rate, lymph node involvement, hormone receptor status and HER2 expression are considered to assess the risk of recurrence (Hong & Xu, 2022). Neoadjuvant therapy is generally favoured for stage II and III tumours, particularly in triple-negative and HER2-positive breast cancers. In both stages of TNBC, the recommended approach consists of a dose-dense chemotherapy using anthracyclines and taxanes, while for stage I of TNBC, an anthracycline-free path might be considered an option (Hong & Xu, 2022).

These treatments have some disadvantages, including the risk for incomplete surgical removal, off-target toxicities, insufficient local drug concentrations at the disease site, and poor drug penetration into the tumours (Bhushan et al., 2021).

1.2.1. Doxorubicin (DOX)

Doxorubicin is an anthracycline antibiotic discovered in the 1960s, being one of the most frequently used chemotherapeutic drugs. DOX became broadly applied in the 1970s as part of chemotherapy treatments for BC and other cancer types, quickly becoming recognized as one of the most effective cytotoxic drugs for treating metastatic breast cancer. Despite its effectiveness, its major drawback is dose-related cardiotoxicity. Researchers have since developed semisynthetic anthracycline alternatives aimed at reducing this risk, though higher overall doses can still cause heart damage. Epirubicin, a variant of doxorubicin, was developed to be less cardiotoxic. Consequently, DOX continues to be a focus of study, with efforts aimed at minimizing its systemic toxicity (Al-malky et al., 2020; Anampa et al., 2015; Nicoletto & Ofner, 2022).

A meta-analysis involving about 1000 women, who were enrolled in randomized clinical trials for early breast cancer, showed that high-dose DOX-based chemotherapy significantly reduced by one third the 10-year breast cancer death rate when compared to

patients who did not undergo chemotherapy. In higher-risk cases, adding taxane (like Paclitaxel, that attaches to microtubules and promotes their stabilization by preventing their breakdown, which causes the cells to become stuck in the mitosis phase, resulting in unfitting chromosome separation due to abnormal, multipolar spindle structures) after administering DOX can lead to even great reductions in risk. The effectiveness of DOX is particularly valuable in patients with TNBC or lymph node involvement (Anampa et al., 2015; Nicoletto & Ofner, 2022).

As previously mentioned, TNBC is defined by the absence of the three key molecular receptors, leaving no available targets for receptor-specific treatments, therefore chemotherapy became the only treatment for nonmetastatic TNBC approved by the Food and Drug Administration (FDA). These tumours are typically flawed in terms of DNA damage repair mechanisms, which is the reason why drugs like DOX are administered – given their nuclear targeting capabilities (Nicoletto & Ofner, 2022).

The standard dosing regimen for DOX as a single agent typically varies from 60 to 75 mg/m^2 and it is administered intravenously every 21 days. When combined with other chemotherapy drugs, the usual dosage lowers to around 40 to 60 mg/m^2 and is administered with a single IV injection every 21 to 28 days. Randomized clinical trials have shown a 4% increase in 10-year survival when anthracyclines like DOX were included in the regimens, comparing to non-anthracycline regimens (Nicoletto & Ofner, 2022).

1.2.1.1. Mechanism of Action of DOX

There are two mechanisms of action considered responsible for the side effects caused by DOX: the first being damage to cell membranes, DNA and proteins caused by free radicals and the second consists of the fact that DOX intercalates into cellular DNA, disrupting DNA repair by specifically targeting topoisomerase IIa (TOP2A) (Al-malky et al., 2020).

In the first process, the DOX is converted into an unstable metabolite, which reverts to DOX, releasing reactive oxygen species (ROS) in the process, which cause cellular damage, including lipid peroxidation, DNA damage and trigger apoptosis (Al-malky et al., 2020). These DOX mechanisms of action are shown in Figure 1.1.

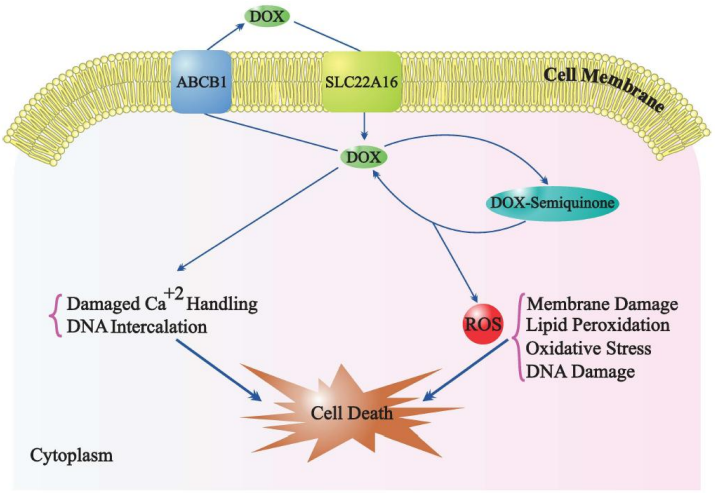

Figure 1.1 – DOX Mechanisms of action illustration (Faraji et al., 2016).

1.2.1.2. Side Effects and Resistance to DOX

Even though DOX is a highly effective drug as a cancer treatment, it is limited by two significant issues: cardiotoxicity and the development of multidrug resistance (MDR) in cancer cells. In many cancer patients, DOX typically causes mild and manageable side effects such as gastrointestinal problems, like nausea, vomiting or diarrhoea, alopecia and oral ulcers (stomatitis). Cardiotoxicity is still the most serious side effect, with reports indicating that approximately 11% of patients treated with DOX experience acute heart-related toxicity. In addition, DOX can negatively affect other organs besides the heart, including kidneys, liver and brain (Al-malky et al., 2020).

Dox-induced cardiotoxicity is notable for its delayed onset, given the fact that the symptoms might emerge only 10 to 15 years after the conclusion of the treatment. Initial signs may include asymptomatic ECG (electrocardiogram) abnormalities, pericarditis or more severe forms of cardiomyopathy – while it is dose-dependent, it can also manifest at lower doses in more vulnerable individuals. Studies have shown that women are more prone to this side effect, with evidence suggesting greater suppression of heart function and a higher likelihood of developing subclinical cardiac damage. Along with gender, age is a significant risk factor, as both younger and older patients tend to me more susceptible to DOX's cardiotoxic effects. It should be noted that pediatric cancer survivors are extremely vulnerable, as the worst cases of cardiotoxicity were seen in these patients, however, it only appears years after ending the treatment. It is estimated that around 60% of pediatric cancer patients receive anthracyclines and 10% of those develop cardiotoxicity within 15 years (Nicoletto & Ofner, 2022).

2. DNA Damage and Repair

DNA is the fundamental carrier of genetic information and is inherently reactive and vulnerable to chemical alterations caused by both internal and external factors. Additionally, the DNA polymerases involved in replication and repair processes occasionally introduce errors, leading to potentially harmful mutations. However, cells possess complex and highly evolved mechanisms, such as DNA repair systems, damage tolerance pathways, cell cycle checkpoints and programmed cell death. These systems function together to minimize the harmful effects of DNA damage. In many cancers, unsurprisingly, both DNA repair and damage tolerance and DNA damage response (DDR) pathways become impaired or deregulated, leading to increased mutagenesis and genomic instability as well as mutation rate and intra-tumour heterogeneity, promoting cancer progression (Chatterjee & Walker, 2017; Kang, 2023).

There are numerous endogenous and exogenous agents that can induce DNA damage – including ultraviolet (UV) light, ionizing radiation (IR) and chemotherapeutic drugs –, that consequently lead to lesions such as mismatches, single-strand breaks (SSBs), double-strand breaks (DSBs), chemical alterations of bases or sugars and inter- or intra-strand crosslinks. If left unrepaired, this damage can result in genomic instability and mutations, which are recognized as key drivers of cancer. To combat these effects, cells have developed a series of protective mechanisms known as the DNA damage response mechanisms– which respond to various forms of DNA damage through processes like signal transduction, transcriptional regulation, cell-cycle checkpoints, apoptosis, damage tolerance pathways and other DNA repair mechanisms (Li et al., 2021).

The DNA damage response provides sufficient time for the specific repair mechanisms to remove the damage based on the type of lesion. There are at least five DNA repair pathways that are operational at various stages of the cell cycle, enabling effective DNA repair: base excision repair (BER), nucleotide excision repair (NER), mismatch repair (MMR), homologous recombination (HR) and non-homologous end joining (NHEJ) (Chatterjee & Walker, 2017).

2.1. Types of DNA Damage in Cancer Cells

DNA damage can be classified into two categories bases on its source: endogenous and exogenous. Most endogenous DNA damage results from DNA's chemical reactivity, as it

undergoes hydrolytic and oxidative reactions with water and reactive oxygen species (ROS), both naturally present in cells. These intrinsic interactions between DNA and surrounding molecules contribute to the development of hereditary disorders and sporadic cancers. In contrast, exogenous DNA damage arises from external environmental, physical or chemical agents, such as UV and ionizing radiation, alkylating agents or crosslinking agents (Chatterjee & Walker, 2017).

Endogenous DNA damages include replication errors, DNA base mismatches and topoisomerase-DNA complexes, spontaneous base deamination, abasic sites, oxidative DNA damage and DNA methylation (Chatterjee & Walker, 2017).

On the other hand, exogenous DNA damage includes IR and UV radiation, along with exogenous chemical agents, toxins and environmental stresses (Chatterjee & Walker, 2017).

2.2. DNA Damage Response

Once DNA damage occurs, specialized sensor proteins trigger the DNA damage response. The DDR, considered an endogenous alarm system, continuously monitors the genome integrity, ensuring accurate genetic information is passed on to daughter cells. Distinct types of DNA lesions trigger distinct alterations in the DNA and cells have developed specialized repair mechanisms tailored to address each type of damage. The recruitment of DDR factors follows a highly regulated, step-by-step process, where they assemble at the damage site in a precise sequence. The mutations in DDR components are linked to cancer predisposition and so, they possess a crucial role in preventing DNA damage-related diseases. However, the DNA repair pathways usually extract most lesions, preventing mutations and the interruption of vital processes like replication, which could otherwise guide to cell death. To provide cells the needed time for DNA repair, the ATM protein adjusts the activity of checkpoint kinases 1 and 2 (CHK1 and CHK2), delaying the cell cycle (Carusillo & Mussolino, 2020; Chatterjee & Walker, 2017).

2.3. DNA Repair Mechanisms

There are at least 5 major types of DNA Repair Mechanisms, which act in order to preserve genomic stability and ensure proper cell function. These pathways identify DNA lesions, signal their presence and restore the integrity of the genetic material through specialized repair processes. When these mechanisms fail, mutations may accumulate,

contributing to cancer development as well as therapy resistance. In Figure 2.1. these mechanisms are illustrated (Chatterjee & Walker, 2017; Pharmaceu Sci et al., 2017).

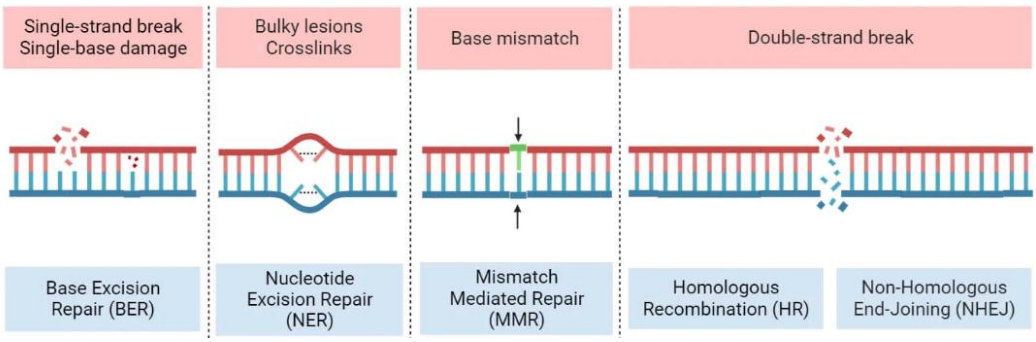

Figure 2.1 – Types of DNA damage and respective repair mechanisms for each (Sanju Tamang, 2023).

2.3.1. Base Excision Repair

Base Excision Repair (BER) is the primary mechanism for fixing damaged DNA bases without cutting the DNA backbone, unlike Nucleotide Excision Repair (NER). The damaged bases are removed by cleaving the N-glycoside bond, leaving the DNA helix intact. This DNA repair pathway fixes oxidative, deamination, alkylation and abasic single-base damage that does not cause meaningful distortion to the DNA helix. BER is mostly active during the G1 phase of the cell cycle. It begins with a chromatin remodelling at the site of damage, followed by the action of four key enzymes that involved in this process: DNA glycosylases, which recognize and remove the faulty base, creating an AP (apurinic or apyrimidinic) site, which is processed by the enzyme AP-endonuclease; then the DNA polymerase fills the gap and ligase seals the strand. Overall, BER is a sequential series of enzyme-driven steps that efficiently restore damaged DNA, as shown in Figure 2.2 (Chatterjee & Walker, 2017; Pharmaceu Sci et al., 2017).

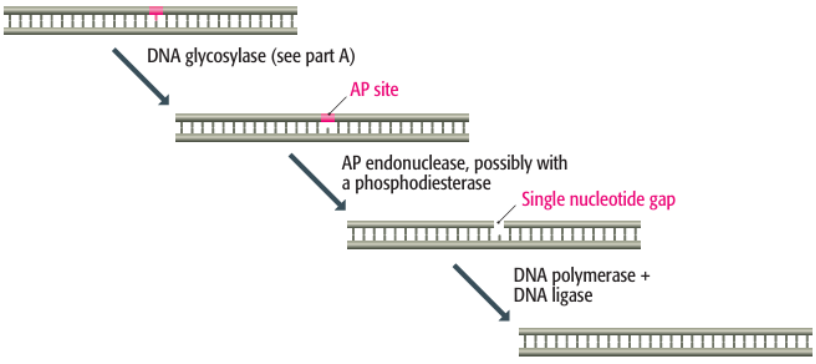

Figure 2.2 – Base Excision Repair pathway (Brown T. A., 2007).

2.3.2. Mismatch Repair

Mismatch Repair (MMR) consists of a repair system that enhances replication accuracy by correcting base pairing errors that occur during DNA replication. It targets mismatched bases and insertion-deletion loops caused by strand slippage in repetitive DNA sequences. MMR also plays a role in meiotic and mitotic recombination, DNA damage signalling and apoptosis (Chatterjee & Walker, 2017).

The MMR process (Figure 2.3) involves three key steps: recognizing the mismatches, excising the error-containing strand and lastly, filling the gap with newly synthesized DNA. Proteins such as Mut S and Mut H, which are produced by the mutator genes, are involved in this process. The Mut S identifies the mismatch and binds the respective region, then the Mut L will recognize the parent strand, forming a loop around the error site and the Mut H cleaves the DNA backbone near the mismatch. Lastly, another protein, the helicase removes the strand, and the DNA polymerase and ligase restore the correct sequence. Defects in MMR results in increased mutation rates, therefore elevating the risk of developing cancer (Pharmaceu Sci et al., 2017).

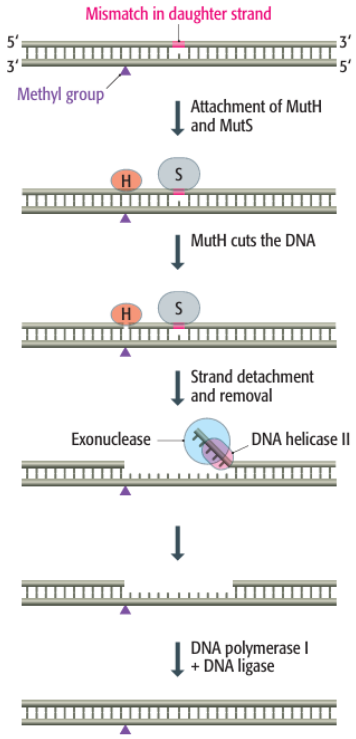

Figure 2.3 – Mismatch Repair pathway (Brown T. A., 2007).

2.3.3. Nucleotide Excision Repair

The Nucleotide Excision Repair (NER) pathway (Figure 2.4) is a complex, multistep process designed to correct various forms of DNA damage, such as lesions caused by UV radiation, reactive chemicals or chemotherapeutic agents that generate bulky DNA adducts. There are two main pathways derived from NER: global genome NER (GG-NER), which identifies and eliminates lesions throughout the entire genome, and the transcription-couple NER (TC-NER), which consists of repairing genes that are actively being transcribed (Chatterjee & Walker, 2017; Hakem, 2008).

The process starts with the detection of the DNA lesion, followed by incisions at the site surrounding the damage, reading to the removal of an oligonucleotide segment containing the lesion. Subsequently, a newly synthesized oligonucleotide – complementary to the existing DNA strand – is connected to fill the resulting gap, completing the repair. Both pathways use several common proteins and follow similar steps in the repair process, however the differ in the initial recognition of the DNA damage, where each pathway uses different protein complexes (Hakem, 2008).

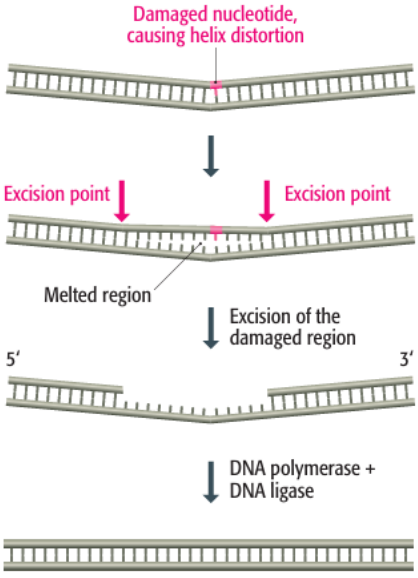

Figure 2.4 – Nucleotide Excision Repair pathway (Brown T. A., 2007).

2.3.4. Double-strand Break Repair

Double Strand Breaks (DSBs) are among the most dangerous types of DNA damage, as even a single DSB can result in cell death. If not properly repaired, DSBs can lead to deletions or chromosomal aberrations, increasing the possibility to have cancer or other

genetic instability syndromes. Therefore, proper DSBs repair is essential for both cell survival and genome stability (Pharmaceu Sci et al., 2017).

There are two distinct pathways capable of repairing DSBs: Homologous Recombination (HR) and Non-Homologous End Joining (NHEJ). HR is an error-free process, as it uses an undamaged sister chromatid as a template for repair, whereas NHEJ is error-prone, directly ligating broken DNA ends. HR is limited to the late S and G2 phases of the cell cycle, while NEHJ operates throughout all phases in mammalian cells. In organisms such as bacteria and yeast, DSBs are mainly repaired by HR, while in mammalian cells, over 90% of DSBs are resolved via the NEHJ mechanism (Figure 2.5). Deficiencies in either pathway can have several consequences, including increased cell death, cell cycle arrest, genomic instability, telomere defects, immunodeficiency, meiotic issues and cancer (Hakem, 2008; Pharmaceu Sci et al., 2017).

2.3.4.1 Non-homologous End Joining

As previously mentioned, NHEJ is the primary pathway for repairing DSBs in mammalian cells and it is particularly active during the G1 phase of the cell cycle, even though it functions along the whole cycle. Defects in NHEJ pathway can result in radiosensitivity, genomic instability, immune deficiencies, growth retardation, impaired embryonic development and an increased risk of cancer complexes (Hakem, 2008).

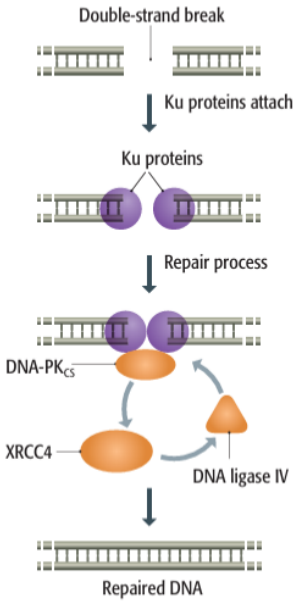

Figure 2.5 – Non-homologous End Joining Repair pathway (Brown T. A., 2007).

2.3.4.2 Homologous Recombination

HR (Figure 2.6) is a pathway that occurs mainly during the S or G2 phase of the cell cycle and repairs approximately 10% of DSBs in mammalian cells. This process is extremely systematic, and any dysfunctions may cause pathologies such as genomic instability, meiotic defects, immunodeficiency and cancer as well as an increase in cell death (Hakem, 2008; Pharmaceu Sci et al., 2017).

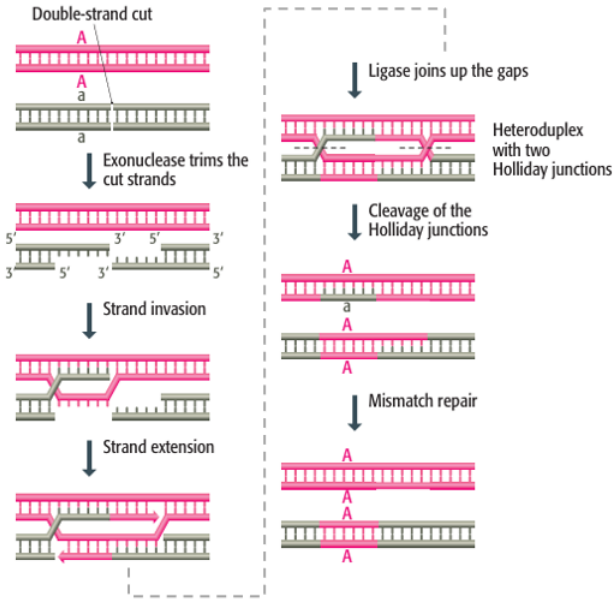

Figure 2.6 – Homologous Recombination Repair pathway (Brown T. A., 2007).

2.4. Role of DNA Repair in Cancer Treatment

Cancer treatments like radio and chemotherapy function by causing direct or indirect DNA damage, inducing eventual cell death. However, cancer cells can also activate DNA repair pathways to resist these treatments and so, combining inhibitors of nuclear or mitochondrial DNA repair pathways with anticancer agents may increase the sensitivity of the tumour cells to these therapies (Li et al., 2021).

Since many cancer cells have flawed DNA repair pathways, they are likely to be more sensitive to DNA-damaging agents. A concept known as “synthetic lethality” exploits this vulnerability by targeting the remaining functional repair pathways to selectively kill cancer cells. Similarly, the heightened sensitivity of tumour cells to oxidative stress due to their rapid replication makes them more dependent on DNA damage prevention pathways. Another common feature of tumour cells is a dysfunctional HR repair pathway and, in such cases, treatments that cause DSBs are often used to induce DNA damage and kill cancer cells (Carusillo & Mussolino, 2020).

Tumour cell's ability to repair damaged DNA is a key factor in developing drug resistance to treatments such as chemo- and radiotherapy, targeted therapy and immunotherapy. In TNBC, low levels of the DNA repair protein 53BP1 – which plays a role in the NHEJ mechanism – were linked to higher rates of local recurrence in patients treated with radiotherapy and breast-conserving surgery. This suggests that this protein could be used as a biomarker for predicting resistance to treatment in those patients. Inhibiting DNA repair kinases has also been shown to prevent breast cancer cells from developing resistance to DOX (Li et al., 2021).

3. Cell Culture Models to Evaluate Genotoxicity

Cell culture is a technique that opens the possibility to better understand cell biology, tissue morphology, drug action or the development of tissue engineering. In cancer investigation, it is crucial to choose the cell culture method in the most appropriate way, in order to allow a better understanding of the tumour biology and optimizing both radio- and chemotherapy (Kapałczyńska et al., 2018).

There are two ways in which cell cultures can be worked out; they can be either under adherent conditions (2D), where the cells are attached to the bottom of a plastic flask or in a suspension, like an agarose gel (3D) – which is the option with more capacity to simulate the natural environment. Nowadays, 2D cell culture is the most frequently applied model, with the 3D technique increasing its popularity gradually (Kapałczyńska et al., 2018).

In the process of the anticancer drugs development, as well as in laboratory attempting to closely replicate the in vivo environment for pre-clinical studies, it is essential for the experimental disease models used to be highly representative of real-life conditions. In breast cancer research, the cell models must reflect the disease's characteristics accurately, including expression of target receptors, drug transporters, critical proteins for cell survival and growth, and the activity of enzymes involved in drug metabolism (Breslin & O'driscoll, 2016).

Normally, the evaluation of anticancer drugs is carried out using different cell lines in 2D cell culture. However, this method does not offer the ability to simulate a microenvironment like the one of a real tumour, which grows three-dimensionally (Imamura et al., 2015). This is major indicator that cultivating cancer cells in 3D is

preferred, given how it is possible to better replicate the in vivo environment when compared to 2D cell culture, as seen in Figure 3.1. In 3D cell culture, the cells can form cell-cell interactions and develop 3D structures, such as spheroids, unlike the monolayer produced by a two-dimensional culture (Breslin & O'driscoll, 2016).

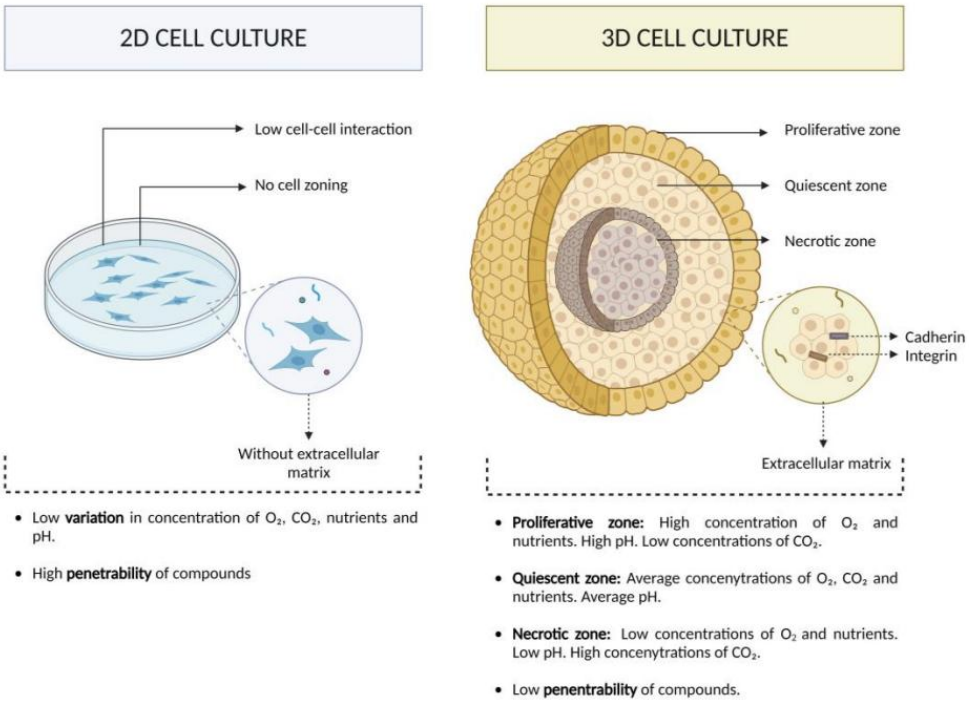

Figure 3.1 - Illustrative diagram of 2D cultured cells and 3D spheroids, presenting the characteristics of each culture type (Garnique et al., 2024).

3.1. 2D Cell Culture

Since early in the 20th century, 2D cell culture has been the most used method to cultivate cells, playing an extremely important role in research (Jensen & Teng, 2020). In 2D cellular culture, the cells grow attached to a flat surface, as a monolayer, as seen on Figure 3.2. This method has some characteristics that are considered beneficial, such as its low cost, easy maintenance and suitability for piloting functional tests (Kapałczyńska et al., 2018).

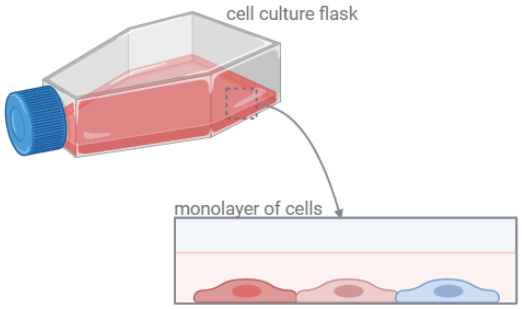

Figure 3.2 - Visual representation of cells growing on a monolayer, in 2D cell culture. (Created with https://www.biorender.com/)

Mainly, the cells provided by this type of culture tend to have a flat and elongated shape, given its bi-dimensionality and the fact that they grow in monolayer, which contributes to the unnatural growth kinetics and cell attachments (Saji Joseph et al., 2019). Besides, most of the cells are in the same stage of the cell cycle, due to their exposure to the medium, from where all of them receive the same quantity of nutrients and growth factors. The resistance of these cells to drugs may be diminished, creating the impression that the administered treatments are highly effective and there is also the fact that the drugs can quickly cause apoptosis in the cells, if exposed for longer periods. Generally, this method has high replicability, and the results are easily interpreted (Jensen & Teng, 2020).

One of the major problems of 2D cell culture is the lack of accuracy when it comes to replicate the microenvironment of the tumours, as well as the natural structures of tissues/tumours. The bi-dimensional technique does not copy the interactions between cells and the extracellular environment that are of extreme importance for processes like cellular proliferation, vitality, cell differentiation, response to stimuli or gene and protein expression (Kapałczyńska et al., 2018).

Upon the isolation of cells from their tissue and later culture in 2D conditions, the morphology of cells and their mode of division changes, leading to the loss of numerous phenotypes. In addition, morphological changes can impact the cells function as well as their organization, secretion and signalling. Given the disrupted interactions between the cells and their environment, adherent cells lose their polarity, affecting their response to some phenomena, like apoptosis. Also, the surface area in contact with the flask and the medium in these type of cells is superior than their contact with neighbour cells, causing them to adopt a form of polarization that does not mimic physiological conditions (Fontoura et al., 2020).The fact that cells grown in monolayer, having unrestricted access

to the medium and its components, such as oxygen, nutrients, metabolites and signal molecules, is another inconvenience of 2D cell culture that results in homogenous growth and proliferation (Duval et al., 2017; Kapałczyńska et al., 2018).

The conditions for 2D cell cultures can differ significantly depending on the cell type, requiring the use of specific culture medium for optimal growth. Laboratories may use various formulations, either prepared in the laboratory or commercially available. Commercial medium is sterile and ready to use, provided in liquid or powder form and typically dissolved in sterile water. Many laboratories prefer to mix commercial components themselves to create a complete culture medium suited for optimal cell growth. These mediums are often supplemented with antibiotics and/or fungicides to prevent contamination. While many continuous mammalians cell lines can thrive on a basic medium like MEM (Minimum Essential Medium) with added serum and antibiotics, most prefer using DMEM (Dulbecco's Modified Eagles Medium), as it supports the growth of mammalian cells more effectively when supplemented with serum and antibiotics (Saji Joseph et al., 2019).

When cells are enough confluent, they need to be passaged, being the first step of this process the detachment of cells from the culture flask, through subjecting them to trypsinization, using trypsin-EDTA (Ethylenediaminetetraacetic Acid). After a short period of time, the cells are loose from the plastic flask and warm medium (around 37ºC) must be added to inactivate the trypsin-EDTA activity. Now, the cells are centrifuged in specific conditions, and the obtained pellet must be divided into new culture flasks with the respective medium for the cell line, also pre-warmed, and the other components, if needed. They must be kept in the incubator at 37ºC, with humidified atmosphere of 5% CO_2 (Saji Joseph et al., 2019).

3.2. 3D Cell Culture

Three-dimensional cell culture was created to enhance the structural integrity and physiological relevance of in vitro experiments. These culture systems offer valuable ways to grow cancer cells, either by themselves or alongside other cell types, in a spatial arrangement that more closely resembles the natural tumour environment. They promote interactions between cells and their surrounding matrix, helping to replicate the physical and biochemical conditions found in real tumours (Kapałczyńska et al., 2018; Saji Joseph et al., 2019).

This technique involves culturing living cells within micro-assembled devices designed to replicate the specific microarchitecture of tissues and organs, being classified based on their preparation method as: suspension cultures on non-adherent plates, cultures in concentrated medium or gel-like substances or culture on scaffolds. In 3D cell cultures, cells grow in their natural three-dimensional configurations, which improves cell-to-cell interactions and intercellular communication networks. Furthermore, the 3D environment facilitates development processes, enabling cells to differentiate into more complex structures (Huang et al., 2020; Kapałczyńska et al., 2018; Saji Joseph et al., 2019).

Scaffold-based culture technologies provide structural support similar to the extracellular matrix (ECM), allowing cells to aggregate, proliferate and migrate. In these methods, cells are implanted into the matrix of the scaffold, and its chemical and physical properties are influenced by the scaffold itself. The scaffold should be biocompatible and able to replicate the native cell functions found within the ECM, while also shaping and defining the function of the incorporated cell culture (Saji Joseph et al., 2019).

Scaffold-free 3D systems promote the formation of multi-cellular aggregates known as spheroids, which can be formed from a variety of cell types. These 3D models possess several key properties, such as the ability to naturally mimic numerous aspects of solid tissues and to originate the ideal physiological cell-to-cell interactions and geometry; they allow cells to form their own ECM components and enhance cell-ECM interactions, while also providing an excellent gradient for the efficient diffusion of growth factors. The concept of 3D spheroids consists of the creation of spheroidal structures in which cells develop into multiple layers, resembling both physical and biochemical characteristics of a solid tumour mass (Kapałczyńska et al., 2018). The size of the spheroids depends on the initial number of seeded cells and can grow to display oxygen and nutrient gradients similar to those in target tissues. They can be easily analysed using light fluorescence and confocal microscopy, which is a significant advantage over other 3D models (Saji Joseph et al., 2019).

Thus, 3D cell culture aims to fix the gap between 2D cell culture and *in vivo* animal models. Furthermore, it has been proved by some studies that in 3D cell culture, the cells response to the drug treatment is more identical to what happens *in vivo* than to 2D cell culture. Besides, it was also shown that cells cultivated by the 3D method are more likely to resist to anticancer drugs when compared to the ones cultured via 2D cell culture. This increased resistance in 3D cultured cells is the result of different factors, including

phenotype and genotype changes, signals from cellular interaction between the ECM and the cells as well as activation of genes involved in cell endurance and drug sensitivity due to inadequate diffusion through the spheroid. Nowadays, tumour spheroids are considered one of the best characterized and mostly used 3D models for studying cancer biology and testing the effects of potential anticancer drugs (Huang et al., 2020; Kapałczyńska et al., 2018; Saji Joseph et al., 2019).

Cell-based assays are a fundamental approach to evaluate the effectiveness of new compounds in the drug discovery process. Therefore, 3D cell culture techniques have been increasingly utilized across different stages of drug discovery, including disease modelling, target identification and validation, compound screening, potency evaluation and toxicity testing. Due to their ability to mimic the behaviour of cells *in vivo*, 3D cultures are particularly useful in the early stages of drug discovery, especially for cytotoxicity tests and flow cytometry assays. Given the distinct behaviour seen on 2D cultured cells and 3D cultured cells, it has been observed that this fact has a particularly significant role in drug discovery, where many promising cancer therapies show favourable results in 2D systems but later encounter failure in clinical trials. By more accurately simulating the natural cellular environment, 3D cell cultures provide better predictive insights into how cells will respond to new treatments, improving the reliability of early-stage drug testing (Saji Joseph et al., 2019).

3.3. Cell Lines

As previously mentioned, breast cancer is extremely heterogeneous, comprising a collection of genetically and epigenetically diseases with diverse clinical presentations. The majority of current knowledge on breast carcinomas comes from both *in vivo* and *in vitro* research using BC cell lines, as they offer an unlimited source of homogenous, self-replicating material through standard media and techniques. While breast cancer cell lines are generally considered to be representative of breast carcinoma, with ER and HER2 being key classifiers, continuous evidence indicates that significant genetic and epigenetic alterations occur during cell line establishment and subsequent passages. This suggests that these cell lines may evolve substantially from the primary tumours (Dai et al., 2017).

There is only a small quantity of cell lines frequently used in research, with lines such as MCF-7, T47D and MDA-MB-231 accounting for over two-thirds of the studies, which

may cause questioning as to whether these limited cell lines represent the vast diversity of breast tumours, each with different clinical outcomes. Therefore, understanding the molecular characteristics of each cell lines and its corresponding tumour subtype is crucial for accurate BC modelling (Dai et al., 2017).

Genetic alterations are more prevalent in BC cell lines than in tumours, with the former exhibiting approximately double the frequency of DNA alterations. This may be since most cell lines originate from invasive, high-grade tumours, which are more prone to accumulating genetic changes during *in vitro* culture. Cell lines may develop alterations not typically found in tumours, possibly derived from the cultivation process or the presence of rare mutations that are difficult to detect in primary tumours. Such changes may lead to phenotypic variations, such as the variable tamoxifen (drug used to treat and prevent BC) sensitivity observed in MCF-7 cell lines. On a molecular scale, key biomarkers and phenotypic traits found in BC cell lines are often mirrored in tumours. Genes associated with ER+ or ER- statuses in cell lines are equally correlated with ER expression in tumours (Dai et al., 2017).

3.3.1. MCF-7

3.3.1.1. Origin and Characteristics

The MCF-7 cell line was established in 1973 at the Michigan Cancer Foundation by Doctor Soule and his colleagues, being nominated after the institution. These cells were isolated from the pleural effusion of a 69-year-old woman with metastatic breast cancer (COMŞA et al., 2015).

MCF-7 is one of the most widely used BC cell lines as it serves as an excellent model for BC studies, including research on anticancer drugs and, over time, this cell line has generated more practical data for patient treatment than any other BC cell line. It is an ER+ and PR+ cell line, being included in the luminal A molecular subtype. Additionally, it is known for being a non-invasive and less aggressive cell line, with generally low metastatic potential (COMŞA et al., 2015).

3.3.1.2. Use in Breast Cancer Research

Diverse MCF-7 variants exhibit divergence at genomic and RNA expression levels. The line is frequently used in research focused on ER+ breast cancer, particularly in studies of acquired anti-estrogen resistance. MCF-7 cells are well-suited for such studies because

they are easy to culture and maintain ER expression even after treatment with anti-hormone therapies. Researchers have created populations of MCF-7 cells adapted to different anti-hormonal environments to study the properties of anti-hormone-resistant breast cancer cells. Eventually, MCF-7 models advanced to *in vivo* systems, which better simulate clinical conditions. These in vivo models allow for a more comprehensive analysis of cancer cell interactions, angiogenesis, metabolism, and respiration – processes that are challenging to evaluate in standard cell culture systems (COMŞA et al., 2015).

MCF-7 cells illustrate several features typical of normal breast epithelial cells, such as the capability to form multicellular 3D aggregate that can develop into spheroids. However, the spheroids derived from the MCF-7 cell line are characterized by a disorganized nuclei, strong cell-to-cell adhesion and lack of lumen formation. Furthermore, MCF-7 spheroids highlight the significance of the microenvironment in tumour metastasis and demonstrate increased resistance to drug treatments compared to cells cultured in a 2D monolayer (COMŞA et al., 2015; Huang et al., 2020).

3.3.2. MCF-10A

3.3.2.1. Origin and Characteristics

The MCF-10 cell line is originated from a patient with fibrocystic disease, with the MCF-10A line emerging naturally during culture. While MCF-10 cells are diploid, MCF-10A cells have a stable, near-diploid chromosome composition, exhibiting mild genetic changes typical of breast epithelial cells that adapt to culture conditions.

These series of cell lines, derived from the MCF-10A cells, offers a valuable model for studying cancer progression in a controlled, molecularly defined way, within the same cellular background. Their capacity to create tissue-like structures in a 3D microenvironment has also been described. In a traditional 2D culture, MCF-10A cells grow in colonies with a cobblestone-like appearance, typically seen on epithelial cells (Imbalzano et al., 2009).

3.3.2.2. Use in Research

When cultured in a 3D reconstituted basement membrane (rBM) environment, MCF-10A cells develop several key features typical of normal breast tissue. This process consists of distinct stages, including initial cell proliferation, cell cycle arrest and, eventually, apoptosis, leading to the formation of a lumen-like space. Moreover, the nuclei of MCF-

10A cells within this 3D environment take on a more organized and differentiated structure, resembling that of mammary epithelial cells in actual breast tissue; more than those cultured in a 2D culture. The spherical cell clusters that form under these conditions resemble normal breast tissue structures, which consist of lobules that connect to the intralobular and interlobular ducts. This cell line offers an excellent model to study how cancer develops at a molecular level, while maintaining a consistent cellular background (Imbalzano et al., 2009).

3.3.3. MDA-MB-231

3.3.3.1. Origin and Characteristics

The MDA-MB-231 cell line is a widely used human breast cancer model, originally derived from the pleural fluid of a 51-year-old Caucasian woman with metastatic mammary adenocarcinoma. Known for its aggressive and invasive characteristics, this epithelial cell line belongs to the TNBC category, as it lacks expression of ER, PR and HER2. This subtype is the most diverse and is often classified into basal A and basal B categories in many studies. The former, also called triple-negative A, is often referred to as basal-like because it is enriched with basal cell markers such as cytokeratin and integrins – these lines resemble the core basal subtype of tumours. In contrast, triple-negative B (basal B) lines, often referred to as the mesenchymal cluster or normal-like/claudin-low, are characterized by the overexpression of genes linked to tumour invasion and aggressiveness (Cailleau,' et al., 1978; Chavez et al., 2010; Dai et al., 2017b; Liu et al., 2003).

3.3.3.2. Use in Triple-Negative Breast Cancer Research

TNBC is a highly aggressive subtype, and the treatment options are quite limited, making it essential to understand its molecular characteristics for the development of new effective therapies. As a result, the MDA-MB-231 cell line has been widely used in studies aimed at identifying potential therapeutic agents for this type of cancer.

In 3D cell cultures, MDA-MB-231 cells display an endothelial-like morphology and exhibit a highly invasive behaviour, forming star-shape extensions that often connect with adjacent cell clusters. This invasive nature is common among claudin-low BC cell lines, which are associated with poor prognosis and higher metastatic potential. Moreover, since 3D cultures enable interactions between the cells and the extracellular matrix, they provide a more physiologically relevant environment for studying cell behaviour and their

response to certain treatments. Thus, this interaction with the extracellular matrix can influence the cells sensitivity to various therapies. (Chavez et al., 2010; Kenny et al., 2007).

It was seen that these cells became more resistant to DOX under 3D culture conditions. Other researchers have also observed greater resistance to chemotherapeutic drugs when breast cancer cells are grown in 3D environments. Although these findings require further investigation, they suggest that using 3D cultures to test therapies may improve the likelihood of preclinical data being effectively applied in clinical practice (Chavez et al., 2010).

4. Comet Assay

4.1. Principle of the Comet Assay

Ostling and Johanson were the first researchers (1984) to quantify DNA damage in cells, developing a new technique now known as "comet assay" or "single cell gel electrophoresis". This original method, however, only measured DSBs, using a microgel electrophoresis system where they firstly fixed mammalian cells in agarose on glass slides, exposing them to X-rays and hydrogen peroxide (H_2O_2), and then lysed the cells using a neutral detergent solution; a low-strength field was applied under neutral conditions, followed by staining the DNA with acridine orange for visualization under the microscope. The DNA migrated toward the anode, with a more significant effect observed in irradiated cells compared to the control group. (Dhawan et al., 2009; Glei et al., 2016; Liao et al., 2009; Møller, 2018).

Over time, the comet assay has been further optimized on various stages, such as lysis and electrophoresis, to accommodate different cell types and forms of DNA damage, becoming a highly sensitive method to evaluate DNA damage and repair in individual cells. Additionally, lesion-specific antibodies or DNA repair enzymes can be used within the assay to identify other types of damage, such as oxidative DNA damage or DNA cross-links. It has become an essential tool in studies of DNA damage and repair, genotoxicity testing and human biomonitoring. The name's analogy is fitting, as the resulting image resembles a comet: the head represents undamaged DNA while the tail contains fragmented or damaged DNA. The quantity of DNA displaced from the comet's head

during electrophoresis correlates with the extent of damage caused by the mutagen being tested (Dhawan et al., 2009; Liao et al., 2009).

This method offers several advantages if compared to other genotoxicity assays, such as remarkable sensitivity, ability to detect even very low levels of DNA damage, low cost and quick and easy application, as well as the fact that it requires a small quantity of cells and it is very adaptable to both proliferating and non-proliferating cells. The produced data at the single-cell level enable rigorous statistical analysis, making the comet assay a reliable tool for evaluating DNA damage across a variety of cell models (Dhawan et al., 2009).

4.2. Methodology of the Comet Assay

To perform a comet assay, it is essential to work with a single-cell suspension. While some samples are already in suspension, there are other, like adherent cells, spheroids, tissues or whole organisms that require enzymatic or mechanical processing in specialized buffers to isolate individual cells. Once the desired cells are isolated, the process follows four main stages, though specific conditions may vary based in the type of sample (Collins et al., 2023).

The essential steps of the comet assay can be summarized as follows, in respective order: cell suspension, chemical treatment, gel preparation, cell lysis, alkaline unwinding, electrophoresis, neutralization, DNA staining and lastly, data analysis (Glei et al., 2016; Lu et al., 2017).

4.2.1. Sample Preparation

Firstly, the slides must be prepared, starting with the slides coating, where 1% agarose is melted so the slides are dipped into it, and cleaned in the bottom side of the slide. The slides must be laid horizontally to dry, forming a transparent agarose film after drying. Then, to prepare the single cell suspension, the cells must be previously cultured and treated in the specific conditions required for each cell line; when ready, they must be exposed to the desired drug or radiation, during the amount of time considered appropriate. The next step is the trypsinization of cells, resulting in the needed cell suspension. This isolated cell suspension is blended with agarose (with the recommended concentration of 0,6% to 0,8%) and spread onto a microscope slide, which is then covered and cooled (at 4ºC) to solidify the agarose into a thin layer of gel. The slides are now

immersed in a lysis solution from 60 minutes (minimum) to overnight, also at 4ºC – this step serves for removing membranes, soluble cell and nuclear components, leaving the DNA attached to the nuclear matrix (Glei et al., 2016; Lu et al., 2017).

4.2.2. Electrophoresis and Staining

Then, for the alkaline comet assay, the slides are removed from de lysis solution and immersed in alkaline electrophoresis solution, again at 4ºC for DNA unwinding, from 20 minutes to 1 hour. The following stage involves the electrophoresis preparation, where the alkaline electrophoresis buffer is added to the tray and the slides are placed inside it; the electrophoresis duration goes from 20 to 40 minutes, at a voltage gradient of 1V/cm. Neutralization comes next and then the slides are ready to be stained. For staining, the slides must be dry so the fluorescent nucleic acid staining solution can be applied onto the dried agarose (Dhawan et al., 2009; Lu et al., 2017).

4.2.3. Image Acquisition and Data Analysis

Finally, the slides are examined using a fluorescence microscope, equipped with appropriate detectors or a digital camera to analyse DNA damage at the individual cell level. While capturing the images from the stained comet slides, it must be guaranteed that the comet tail is horizontally distributed: tails should originate from left to right. The images must be saved in the desired format (TIFF, CZI, etc) and loaded to the software in use. The software determines parameters such as length of the comet tail, the percentage of the tailed DNA and the tail moment (TM) and at least 50 cells per treatment must be analysed (Dhawan et al., 2009; Lu et al., 2017).

4.3. Limitations and Challenges of the Comet Assay

Although the comet assay offers numerous advantages, it does have some limitations. One obstacle is its inability to detect epigenetic mechanisms of DNA damage, such as disruptions to cell-cycle checkpoints. Additionally, challenges include the use of small cell samples – which can introduce bias –, variability in technical execution and interpretation, as well as the reliance on single-cell data (Dhawan et al., 2009).

A major technical challenge lies in scoring the comets, as DNA damage is judged from its migration, which can be evaluated through automated image analysis or visual inspection. However, different variables – such as tail length, tail intensity and tail

moment – present results in various units that are not easily comparable (Collins et al., 2023).

In conclusion, despite these limitations – including technical variability, the challenge of interpreting results across different laboratories, and the inherent complexity in scoring comets – the comet assay remains a highly valuable tool. It is extensively used for assessing DNA damage and repair across a wide range of biological models (Collins et al., 2023; Dhawan et al., 2009).

5. Materials and Methods

5.1. Cell culture

There were used three types of cell lines in this project: MCF-7, MCF-10A and MDA-MB-231, both in 2D and 3D culture.

5.1.1. 2D cell culture

All cell-lines are kept at -80ºC, therefore, the first step of the 2D cell culture process is to defrost them. They are conserved in 1 millilitre (ml) vials, each containing 500 microliters (µl) of Fetal Bovine Serum (FBS – from Thermo Fisher Scientific Inc.), 100 µl of Dimethyl Sulfoxide (DMSO) and 400 µl of the previously trypsinized cell suspension.

To do so, it should be added medium (specified to each cell line) to the vial content, in a falcon – around 5ml – and centrifuge for 5 minutes, at 20ºC and 1000 rpm (revolutions per minute). The remaining pellet is transferred to a T25 (25 cm^3) flask, prepared with the required conditions for each cell-line and quarantined for at least a week in a specified quarantine incubator, at 37ºC and 5% CO_2.

The medium must be changed each 2 days and, when the required confluence is reached (around 70-80%), the cells can be passaged, either to a T75 (75 cm^3) or a T175 (175 cm^3) flask (both techniques occur in biosafety cabins). This process consists of trypsinizing the cells, recuring to a mixture of 2,25 ml of Versene, 250 µl of Trypsin (Sigma-Aldrich) and 20 µl of Sodium Bicarbonate – that is, if the flask is a T75; if it is a T175, the quantities must be doubled – and letting it incubate at 37ºC from 5 to 10 minutes – it should be noted that the cells were previously washed with Versene and Sodium Bicarbonate. Then, when the cells are no longer attached to the culture flask, 7,5 ml of medium is added (3 times

the quantity of Versene-trypsin) and the suspension is transferred to a falcon and centrifuged for 5 minutes, at 20ºC and 1000 rpm. The medium is discarded, and the obtained pellet can be divided into the new flasks – in this part of the process, around 500 µl to 1 ml of medium can be added to the pellet, if needed, to resuspend the cells –, already prepared with the specified mediums and complements for each cell-line.

In between processes the flasks must be kept in incubators (BINDER, BD-S 115) at 37ºC and 5% CO_2, in order to keep the cells in a controlled and warm environment. The cells must be passed at least 3 times before being used in the comet assay.

Both MCF-7 and MDA-MB-231 cell-lines require the same type of medium, being used the Dulbecco′s Modified Eagle′s Medium – low glucose (DMEM LG), from Sigma Aldrich, complemented with 10% of FBS and 1% of Penicilin-Streptomycin (Penstrep). Given some technical problems, this medium was later replaced with Dulbecco′s Modified Eagle′s Medium – high glucose (DMEM HG), supplemented equally to the DMEM LG and, as no apparent differences were seen on both cell-lines, this medium was used until the end of the procedures. The MCF-7 cell-line must be also supplemented with insulin, in a 1:1000 proportion.

The MCF-10A cell-line is supplement with DMEM F-12 (Nutrient Mixture F12) medium (Sigma Aldrich), enriched with 5% Horse Serum (HS), 1% of Penstrep, 0,1% of Epidermal Growth Factor (EGF) and 0,05% of Hydrocortisone. In addition, it is also supplemented with insulin (1:1000 proportion) and Choleric Toxin (CTx) (1:100 proportion).

5.1.2. 3D cell culture

The preparation for 3D cell culture is identical to the 2D cell culture process, and so, all the previous mentioned steps must be accomplished in order for the cells to be ready to use in three-dimensions. The 3D culture method consisted of the use of moulds (3D Petri Dish – micro-mould spheroids - size L, 5 x 7 array, Sigma Aldrich), following the "Microtissues – natural 3D: Casting, Equilibrating and Seeding the 3D Petri Dish" protocol (Casting, Equilibrating and Seeding the 3D Petri Dish, n.d.).

The first step of the process consists in autoclaving the needed material, including the 3D Petri Dishes (previously washed with distilled water (dH_2O)), 1g of agarose powder (in a 100ml glass bottle) and 0,45g of Sodium Chloride (NaCl) – in order to make a 0,9% (w/v)

NaCl solution. In a biosafety cabinet, 50ml of double-distilled water (ddH_2O) is joined to the NaCl and then, this solution is added to the bottle containing the sterile agarose powder, swirling the bottle to mix the materials. The lid of the bottle should be screwed but still loose, because the next step happens outside the biosafety cabinet, recurring to the microwave oven in order to boil and dissolve the agarose.

Again, in the biosafety cabinet, using aseptic technique, the agarose must be cooled to about 60-70ºC. Using a micropipette, 330 µl of the melted agarose is pipetted into the 35 wells micro-moulds, ensuring no bubbles are formed. When the agarose is ready, the process showed in Figure 5.1 must be carefully performed into a 24 well tissue culture plate, slightly flexing the mould so the gelled agarose (Figure 5.2) falls easily.

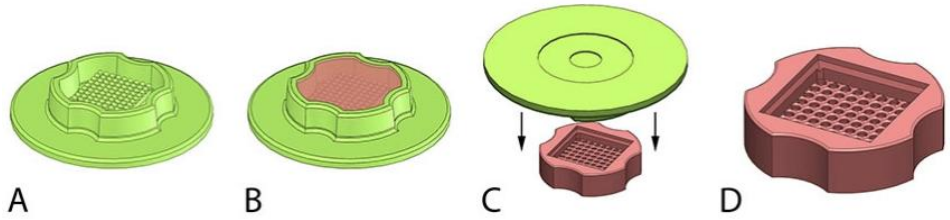

Figure 5.1 - Unmoulding process of the jellified agarose. *(*Casting, Equilibrating and Seeding the 3D Petri Dish*, n.d.)*

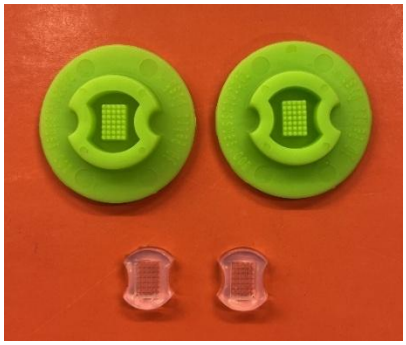

Figure 5.2 - Petri Dish 3D and respective agarose gel moulds.

At this point, and when the needed quantity of micro-moulds is placed on the tissue culture plate, they must be equilibrated. To do so, 1 ml of medium is added to each well and the plate is incubated for at least 15 minutes. This step is repeated one more time, so the equilibrating process is complete.

In the meanwhile, the cells are trypsinized, counted and the desired cell seeding number is prepared in the specified volume for the 3D micro-moulds. On this step, it must be taken to account that, as the produced spheroids should be developed with around 2000

cells each – therefore 70000 cells per mould –, the prepared cell suspension must be calculated so that 75 µl correspond to that required cell quantity.

On this stage of the process, the medium used to equilibrate the moulds is removed, both on the outside and the inside part of the micro-mould. The 75 µl of cell suspension can now be pipetted into the 3D Petri Dish. The cells must be given around 10 minutes to settle into the micro-moulds and then, 1ml of medium is carefully added per well. It should be noted that, if the cell-line in use is either MCF-7 or MCF-10A, the medium supplemented with insulin or both insulin and CTx, respectively, is to be previously prepared.

The developing spheroids must be kept in a controlled environment, incubated at 37ºC and 5% CO_2. The medium changes occur every 3 days and, on the eighth day of culture, the spheroids are ready to be subjected to the comet assay process.

5.2. Comet assay procedure

The primary step that should be followed is the preparation of the solutions that will be further needed. All the specifications for each solution are presented on Table 4 and Table 5, situated in the annexes.

Along with the solutions, one of the first steps on the comet assay, for both 2D and 3D culture is to prepare the slides. A layer of 1% Agarose (prepared with ddH_2O) is added to the slides (previously kept at 4ºC) with a submersion method and they are stored in a closed box at room temperature. This step must be made with some days in advance, so the slides have time to dry before use. Additionally, in case of need, there is also the option to use pre-coated slides.

5.2.1. Comet assay – 2D

When working on 2D culture, the first step is to passage the cells into a 12 well tissue culture plate, that is, trypsinizing the grown cells recurring to the same process as if they were being passaged to a common culture flask. After trypsinization and centrifugation, the medium is discarded, and the remaining pellet must be resuspended so that 10 µl of cell suspension can be used to count the cells. For that, 10 µl of Trypan Blue is added to the cell suspension and 10 µl of this cell mixture is used, recurring to the Invitrogen Countess 3 counter (Thermo Fisher Scientific, Invitrogen Countess 3 FL). The

calculations were made aiming for 70000 cells in each well and, after counting and rearrangement of the cell suspension, the cells were placed into the wells, with 1ml of the required medium and supplements for each cell line. The plate was kept, for 24 hours, at 37ºC and 5% CO_2.

After that period, the following step was to apply the desired chemicals to the cells. In this case, it was used DOX with concentrations of 0,4mM (milli-Molar) for 1µM DOX treatment and 2mM for treatments at 2µM and 5µM; as well as H_2O_2 (Hydrogen Peroxide) in concentrations of 25µM and 50µM (used as positive control) – the H_2O_2 was diluted in a proportion of 1:1000, being used at 0,01M. As a negative control, 2 wells were left only with cells. The procedure was carried with duplicates; therefore, each treatment was placed in 2 wells. The chemicals were left to act for 3 hours, incubated at 37ºC and 5% CO_2.

The next step consisted of a normal trypsinization process, applying 200µl of Trypsin mixed with Versene and Sodium Bicarbonate, leaving it to react from 10-15 minutes. Then, 800 µl of medium is added and each cell suspension is transferred to identified Eppendorf's and those are centrifuged for 5 minutes, 20ºC and 2000rpm. Following that (no longer in the biosafety cabin), the medium is discarded, and the samples are washed with PBS (Phosphate-Buffered Saline) and centrifuged one more time, with the same conditions. The supernatant is thrown way, using the inversion method, leaving the pellet.

This pellet is resuspended with 150µl of 0,5% Low Melting Point (LMP) Agarose and 75µl of this suspension is applied to the previously coated slides, placing the cover slips on top of the slides. The slides are left to dry, horizontally, for 20 minutes at 4ºC. Afterward, the cover slips are carefully removed, and the slides are stored in cold coupling-jars (4ºC) immersed in lysis buffer. They are stored overnight at 4ºC.

The next day, the lysis buffer is poured out and autoclaved ddH_2O (4ºC) is added to wash, discarding it right away and adding new water, leaving it for 10 minutes. In this period, 2000ml of electrophoresis buffer is prepared with 10ml of 2000mM EDTA and 60 ml of 10 Sodium Hydroxide (NaOH). At this point, the ddH_2O is discarded and the electrophoresis buffer is added to the slides, for 20 minutes at 4ºC.

In the meantime, the electrophoresis chamber (BRL Horizon 20.25 – Horizontal Gel Electrophoresis System Cat. No. 1069BD) is prepared with the cold electrophoresis buffer

and then, the slides are placed in the chamber. The electrophoresis runs for 20 minutes at 25V (Volts) and 400mA (milli-Amperes) (BioRad, POWER PAC 300).

Following that, the slides are placed horizontally in absorbent paper, and, with the help of a Pasteur pipette, neutralization buffer is added and left to act for 5 minutes, repeating this step 3 times. The buffer is removed with water, and the slides fixation proceeds by first applying 50% Ethanol, leaving it for 5 minutes and repeating the process two more times, using 75% Ethanol and 100% Ethanol. The slides should be left to dry horizontally and kept in a closed box until the next step.

At this phase, if the slides are to be coloured the day after electrophoresis, it is only needed to stain them with GelRed (3 times concentrated), applying 80µl of the solution to each slide and observing them on the microscope (ZEISS Axio Imager Z2 model).

The objective was to have at least 200 cells per each slide, so they could be analysed using the CometScore software. To evaluate the level of DNA damage, the percentage of DNA located in the tail of the comets, known as %Tail DNA, was measured.

5.2.2. Comet assay – 3D

The procedure for the 3D comet assay is identical to the 2D comet assay procedure, except for the trypsinization method. That is due to the fact that the protocol used to trypsinize spheroids is different from the one used on adherent cells. The guideline followed for the first 3d experiments is the "Microtissues natural 3D: Harvesting Multi-cellular Microtissues from the 3D Petri Dish" ("Harvesting Multi-Cellular Microtissues from the 3D Petri Dish," n.d.), while for the second experiments, this method suffered some changes, in order to optimize the assay – given the lack of results obtained on the first ones.

On the eighth day of culture, the spheroids are ready to be submitted to the chemical treatment, which is precisely the same used in 2D culture, including the incubation period. After that (outside of the safety cabin), the first step is to remove the cell culture medium from the wells. On a new 12 well plate is added 1ml of cell culture medium or PBS (PBS was used, in this case). At this point, the 3D Petri Dish are carefully transferred, recurring to a sterile tweezer, to the new plate, inverting them so the well side is facing the bottom of the plate. The cell culture plates are centrifuged (Tehtnica, CENTRIC 322A) for 5 minutes at 2000rpm.

After centrifugation, the empty moulds are removed, and the spheroids are now liberated on the PBS. Carefully, the PBS must be also removed, leaving only the spheroids on each well – this step could potentially contribute to cell loss, which is why it was changed for the second experiments, where both the PBS and the spheroids were transferred to Eppendorf's, where the trypsinization later occurred. Following, 200µl of the Versene, Trypsin and Sodium Bicarbonate mixture is applied in each well and left to act from 5-10 minutes. To inhibit the trypsin action, 800µl of PBS are added to each well and then, each cell suspension is transferred to identified Eppendorf's, and these are centrifuged for 5 minutes, at 2000rpm and 20ºC. In 2D, the cells are washed with PBS at this stage, but this step was considered unnecessary as the spheroids had already been centrifuged with PBS one time.

The following steps are equal do the ones applied in the comet assay procedure in two-dimensions.

5.2.3. Data Analysis

In order to obtain the data, the program CometScore, by Rex Hover, was used to read every cell, one by one, from all different concentrations and cell lines. The aim was to quantify the percentage of DNA in the comet tails for a minimum of 200 cells at each concentration. However, given that this assay is subject to certain fluctuations in the number of cells per slide, the actual number of cells analysed per sample showed some variation.

With that in mind, the assays that were successfully performed showed a larger quantity of cells and it could vary from the minimum of cells required to around 900-1400 cells; in cases where errors occurred during either the cell culture or the comet assay procedure, the slides potentially failed to reach the required minimum number of cells, or in some instances contained no analysable cells at all.

At the end of the analysis, the software generates an Excel file containing numerous variables, of which only the percentage of DNA in the comet tail was used. All data corresponding to this variable were subsequently transferred to a new Excel file, organized according to culture dimensionality, cell line, and the respective treatment condition. Graphs were generated using GraphPad Prism (version 10.6.0).

As for the spheroids morphological analysis, the program CellProfiler (version 4.2.8) was used. Each spheroid was manually delineated and the commands used to provide the required values were “Measure Object Size Shape” and “Calculate Math”; on the latter, the specified variables were chosen, in particular: spheroid area, maximum and minimum Feret diameter, solidity, compactness and eccentricity.

6. Results and Discussion

This section reports the obtained results from the morphological characterization of the spheroids formed by the three cell lines previously mentioned as well as the analysis of DNA damage assessed by the comet assay. Quantitative data on spheroid morphology and the percentage of DNA in comet tails are presented, allowing intercellular comparisons.

6.1. Morphological Characterization of Spheroids

6.1.1. MCF-10A Spheroids

Spheroids derived from the MCF-10A cell line exhibited substantial changes between day 1 and day 3, where it was clearly possible to observe that this cell line produces spheroids with a well-defined morphology, as shown in Figure 6.1. By the final day of culture (day 8), the spheroids morphology remained similar to that of days 3 and 6, continuing to display a very well-defined structure as well as high cellular compactness.

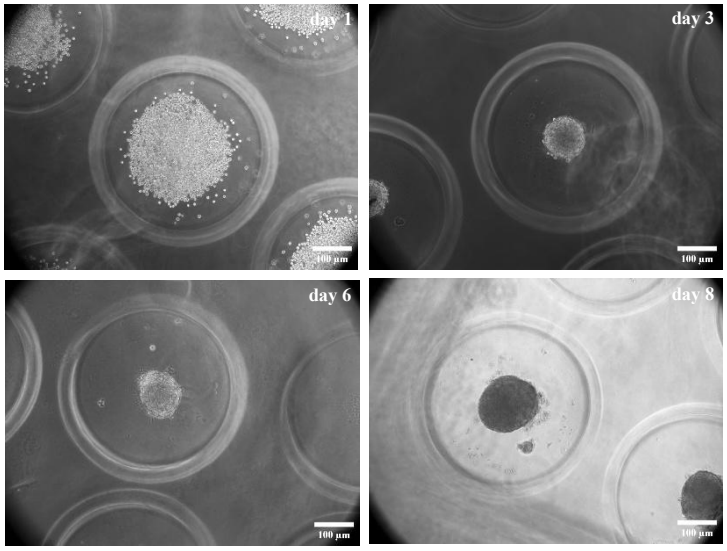

Figure 6.1 - Growth of MCF-10A cell line spheroids over 8 days under the previously indicated conditions, acquired using a 10× objective. Scale: 100µm.

Regarding the morphological analysis of spheroids performed after treatment, those derived from this cell line showed slight differences at the two time points evaluated (1h and 3h). As shown on Figures 6.2 and 6.3, an apparent reduction in spheroid area was observed over time.

The negative control exhibited the smallest spheroid area (mean~10.025µm^2), which may indicate that untreated spheroids maintain a relatively constant and smaller size. Upon treatment with DOX, an initial increase in spheroid was observed after 1h of exposure,

followed by a progressive reduction over time. This transient enlargement may reflect cellular swelling induced by DOX as a consequence of membrane compromise due to cellular damage, which is later followed by a decrease in area, consistent with the cytotoxic effects of the drug. At higher DOX concentration, the progressive decrease continued over time, suggesting that the drug leads to a loss of spheroid size, potentially due to decreased cell-cell adhesion, as DOX has been reported to modify cell membrane characteristics (Ncube et al., 2023).

For H_2O_2, the effect was not as linear. The lower concentration (25µM) caused a reduction in spheroid area as early as 1 hour on treatment, which was maintained at 3h. However, the higher concentration (50µM) initially resulted in larger areas compared to 25µM and remained relatively high even after 3h. This suggests that higher concentrations of hydrogen peroxide may induce a distinct type of cellular damage that does not necessarily translate into a rapid reduction of the spheroid area. Overall, the progressive reduction on this variable over time indicates the spheroids capacity do remain stable as a response to treatment.

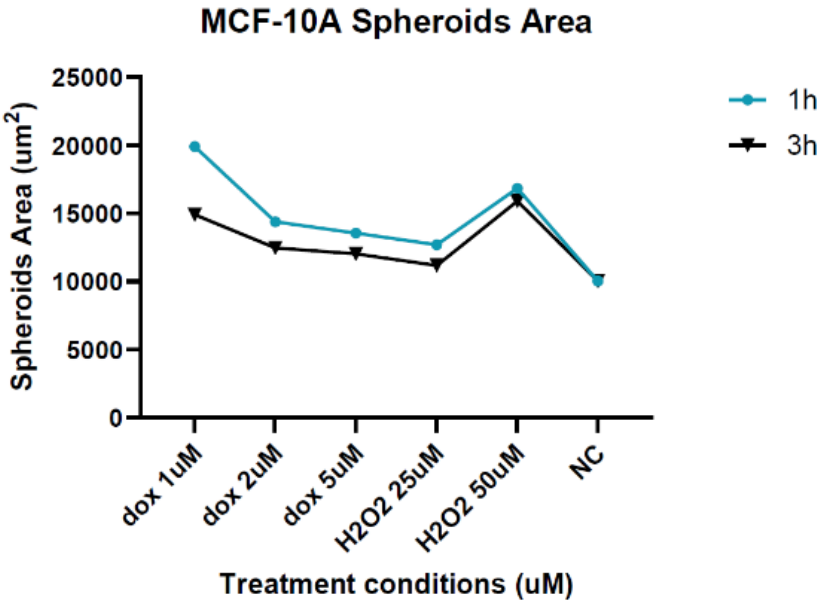

Figure 6.2 – MCF-10A spheroids area: comparison between 1 hour and 3 hours after treatment, for each different condition.

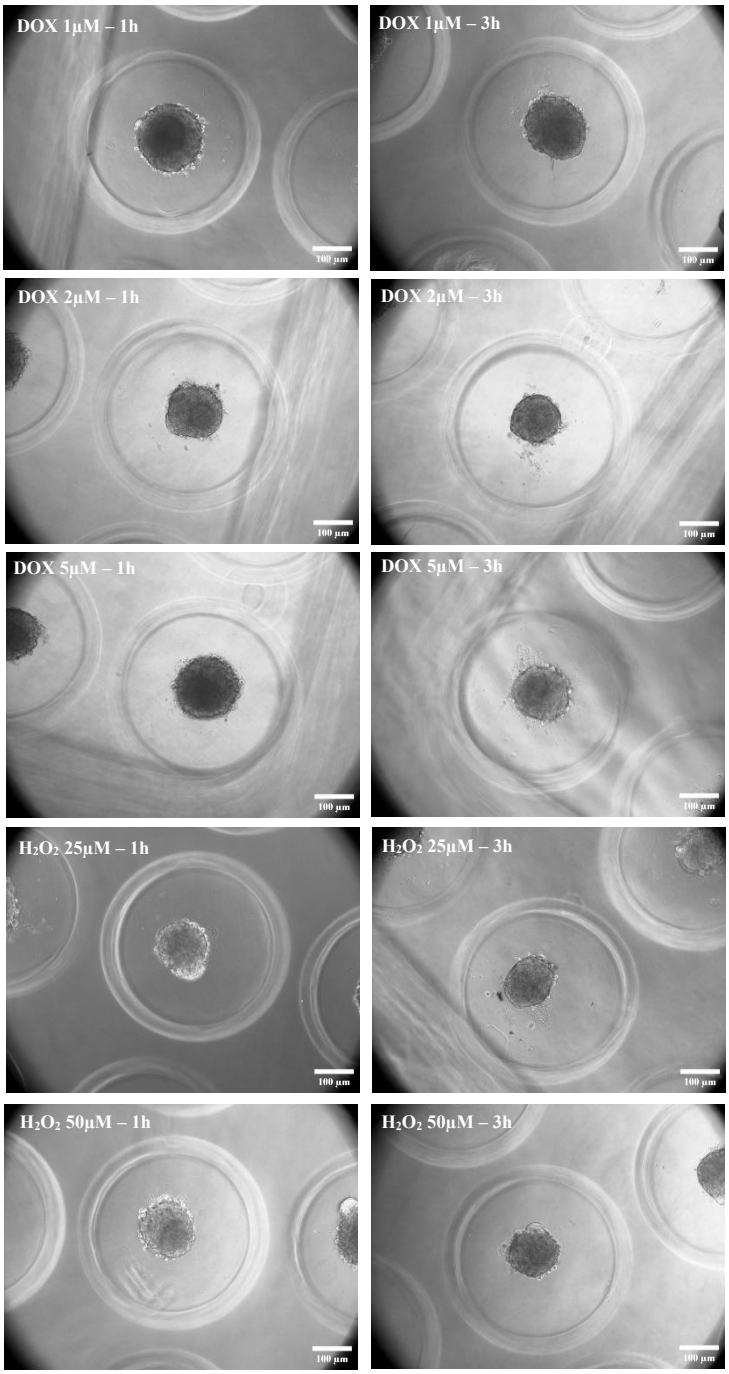

Figure 6.3 – MCF-10A spheroids morphology after 1h and 3h of exposure to each treatment condition. Microscopy images obtained through 10x ampliation, scale: 100µm.

6.1.2. MCF-7 Spheroids

The microscopy images of MCF-7 spheroids (Figure 6.4) revealed a progressive increase in morphological irregularity throughout the culture period. The spheroids exhibited poorly defined borders and reduced compactness over time, particularly in the centre region, which may indicate cellular necrosis. By the final day of culture, spheroids had

clearly lost structural cohesion and displayed higher heterogeneity, consistent with cell death likely caused by the limited diffusion of oxygen and nutrients from the spheroid's periphery to the core; in line with this, peripheral cells continued to proliferate, as reflected by the increased irregularity on the spheroid's edges.

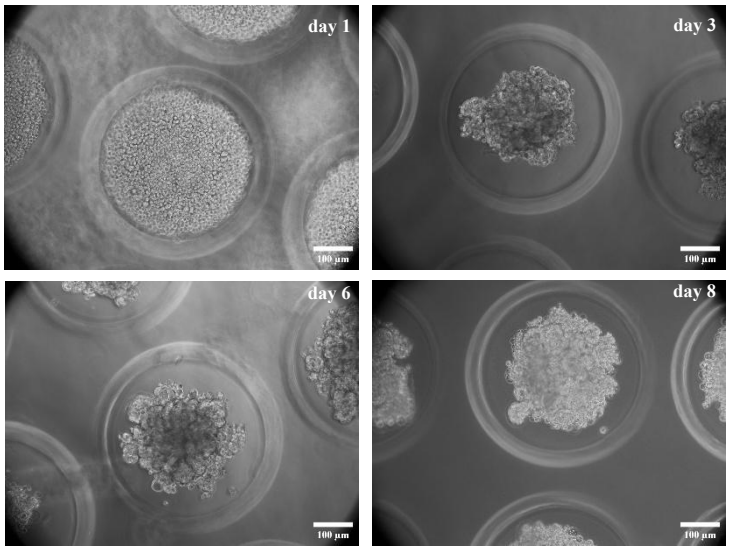

Figure 6.4 - Growth of MCF-7 cell line spheroids over 8 days under the previously indicated conditions, acquired using a 10× objective. Scale: 100 µm.

The analysis of spheroid area (Figure 6.5) in MCF-7 cells revealed distinct responses to the applied treatments, highlighting both dose and time dependent effects. Negative control maintained the smallest and most stable spheroids dimensions, suggesting that in the absence of treatment these structures remain compact and don't present relevant morphological changes.

Spheroids with DOX exposure at 2µM displayed a temporary increase in area after 1h of treatment, which may be triggered by cellular swelling caused by membrane compromise, a phenomenon often associated with early cytotoxic events. This increase was followed by a reduction after 3h, indicating the progression towards cytotoxicity. In contrast, treatment with 1µM and 5µM resulted in a progressive decrease of area from the first timepoint. At 1µM, the spheroids exhibited smaller dimensions compared to the NC, becoming more pronounced after 3h. This suggests that even low doses of DOX have the capability to trigger early structural alterations, most likely linked to initial cytotoxic effects, without evidence of cellular swelling. At the highest concentration, a rapid reduction in spheroid area was observed. Spheroids exposed to DOX 5µM showed a decrease in size after 1h, which was further intensified after 3h of treatment. The absence of an initial swelling phase and the strong reduction over time indicate a rapid and

effective cytotoxic effect of the treatment, possibly driven by higher intracellular accumulation of the drug, leading to apparent loss of cell viability and disruption of the spheroid integrity. The spatial heterogeneity observed (Figure 6.6) within the spheroids may also have contributed to the diminished effectiveness of DOX, as this agent usually targets proliferating cells first. The outer layer, characterized by higher proliferation rates was apparently more responsive to the drug, as suggested by the reduction in spheroid size (Ncube et al., 2023).

As for the treatment of H_2O_2, at 25 µM, the decrease was moderate and relatively stable between hour 1 and hour 3, suggesting a sustained but less aggressive oxidative effect. In contrast, exposure to H_2O_2 50 µM caused a rapid decrease in spheroid area, with a reduction of more than 25% compared to the negative control within the first hour. This decline indicates a strong cytotoxic effect, coherent with the ability of H_2O_2 to generate ROS – although excessive ROS production can promote cellular proliferation and work as a redox signalling molecule under physiological conditions, it also causes genetic instability and is able to activate apoptotic pathways under oxidative stress, where it is produced in excess (Ali et al., 2024).

The immediate impact of high H_2O_2 concentrations suggests that oxidative stress exerts a violent effect on spheroid morphology, distinct from the more progressive response to the DOX treatment. Severe exposure to moderate H_2O_2 concentrations may induce apoptosis, whereas higher doses may cause necrosis. While DOX exposure was associated with a transient swelling effect followed by size reduction, H_2O_2 triggered an early collapse of spheroid architecture without evidence of initial swelling. This difference likely reflects the distinct mechanism of action from both drugs: H_2O_2 tends to provoke direct oxidative

stress whereas DOX tends to trigger membrane damage (Ali et al., 2024; Ncube et al., 2023).

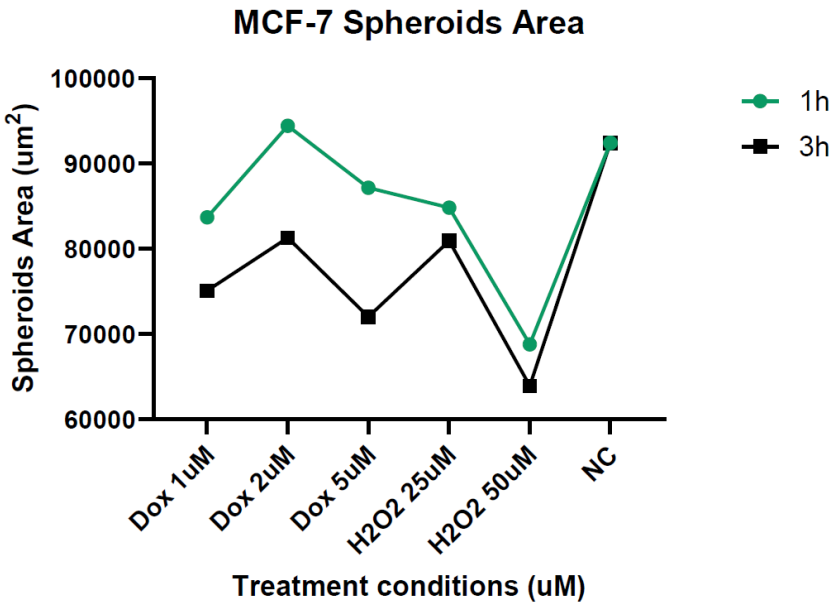

Figure 6.5 - MCF-7 spheroids area: comparison between 1 hour and 3 hours after treatment, for each different condition.

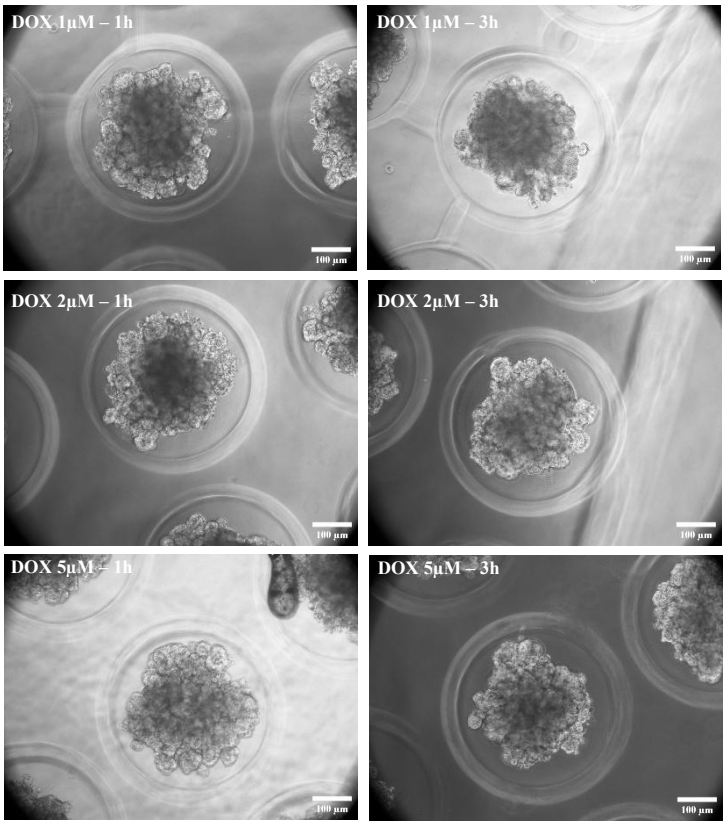

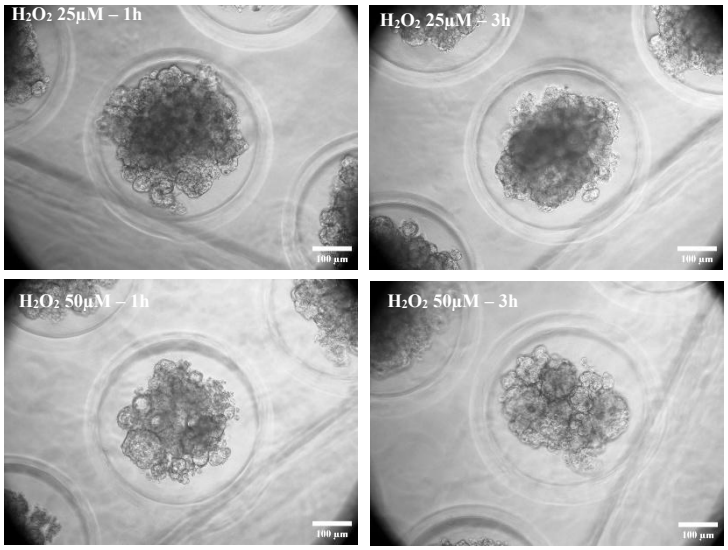

Figure 6.6 - MCF-7 spheroids morphology after 1h and 3h of exposure to each treatment condition. Microscopy images obtained through 10x ampliation, scale: 100µm.

6.1.3. MDA-MB-231 Spheroids

In the case of MDA-MB-231, it should be noted that the spheroids that were analysed for the morphological study were substantially smaller (Figure 6.9) than those presented in Figure 6.7, which originated from another assay, as was performed more than one experiment for each cell line. This discrepancy may reflect some procedure differences, such as seeding density or culture conditions rather than a true biological inconsistency. All comparisons presented in this section were conducted within the same experimental run and using the same image-processing method; thus, relative changes across treatments and time points remain valid and interpretable. The reduced absolute size is, however, recognized as a limitation of the experiment. To enhance the analysis coherence, the results were normalised to the corresponding negative control and subjected to appropriate statistical testing.

On Figure 6.7, which illustrates the growth of MDA-MB-231 spheroids from day 1 to day 8, it is possible to see that by day 3, the structures are more irregular, displaying partial disaggregation and poorly defined edges. By day 8, the irregularities are even more evident, with spheroids displaying disrupted peripheries and an overall less uniform architecture, suggesting instability of the spheroid over time. This progressive loss of compactness and the irregular morphologies observed from day 3 onwards are consistent with the invasive phenotype of this cell line, which is known to form spheroids that are less cohesive and structurally unstable, as this cell line has previously exhibited malignant

characteristics close to those of one *in vivo* tumour, like reduced proliferation, hypoxia and higher tolerance against toxic agents (Huang et al., 2020).

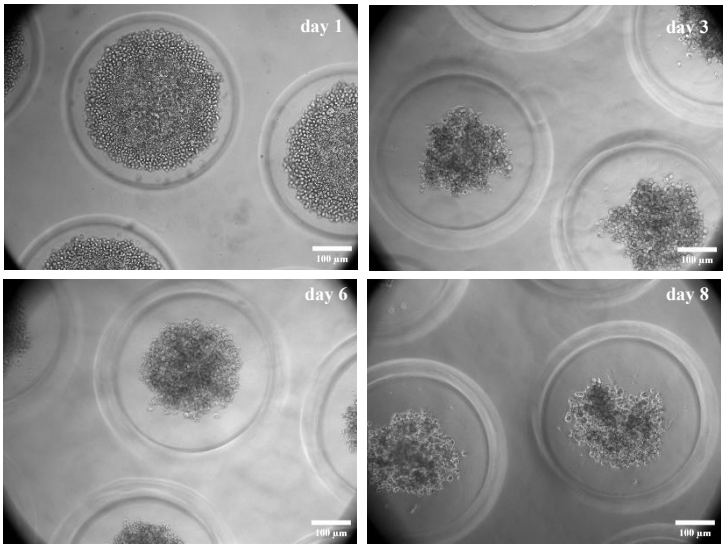

Figure 6.7 - Growth of MDA-MB-231 cell line spheroids over 8 days under the previously indicated conditions, acquired using a 10× objective.

Given the previously mentioned limitations, the morphological analysis is interpreted with caution, focusing primarily on relative differences between treatments and timepoints rather that absolute size values.

On DOX 1µM treatment, the spheroids area (Figure 6.8) at 1h is substantially larger than the negative control, with a partial decrease by the 3h timepoint, which might be consistent with a transient enlargement followed by limited recovery or early cytotoxic progression. However, for DOX 2µM the response is quite different. It shows pronounced reductions at both timepoints, indicating an apparent increase in the cytotoxic effect of the drug. As for the treatment with DOX 5µM, the spheroids area is considerably elevated, when comparing to NC, both at 1h and 3h after treatment application. This could mean substantial swelling or structural reorganization rather than immediate collapse. In addition, Figure 6.10 shows that both DOX 1µM and DOX 5µM exhibited poorly defined borders. It is clear that peripheral cells continued to proliferate and eventually lost cell cohesion, forming an extremely irregular border, which might be the cause for the increase of area on these two treatments(Ncube et al., 2023).

Hydrogen peroxide performed a dose and time dependent response, where at 25µM, an initial reduction in area at 1h may suggest early cytotoxic effects, followed by a slight increase by 3h, likely reflecting transient swelling or loss of cell-cell contact. At a concentration of 50µM, that same initial reduction occurs, although not as evident, and is

followed by a pronounced increase at 3h, possibly indicating structural reorganization induced by oxidative stress. Another potential factor for this behaviour could be the inherently rapid and efficient mechanisms of response to damage of MDA-MB-231 cells. These cells are known to activate antioxidant systems and DDRs more rapidly that less aggressive cell lines, allowing them to withstand oxidative stress; although ROS strongly activates DDR pathways, the strong antioxidant defense and efficient DDR activation in these cells demonstrate their capacity to counteract and overcome ROS-induced damage. This ability may be the cause of resistance to high concentrations of H_2O_2 and the subsequent structural reorganization and swelling observed at later timepoints. Peripheral cell growth is also observed on H_2O_2 treatments, which may further contribute to the increase seen in the spheroids area (Ali et al., 2024; Dong et al., 2025).

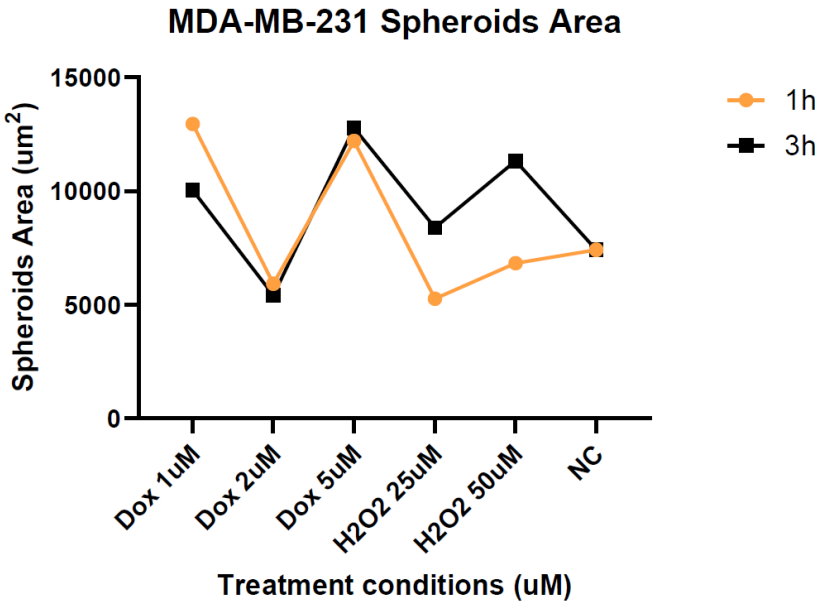

Figure 6.8 – MDA-MB-231 spheroids area: comparison between 1 hour and 3 hours after treatment, for each different condition.

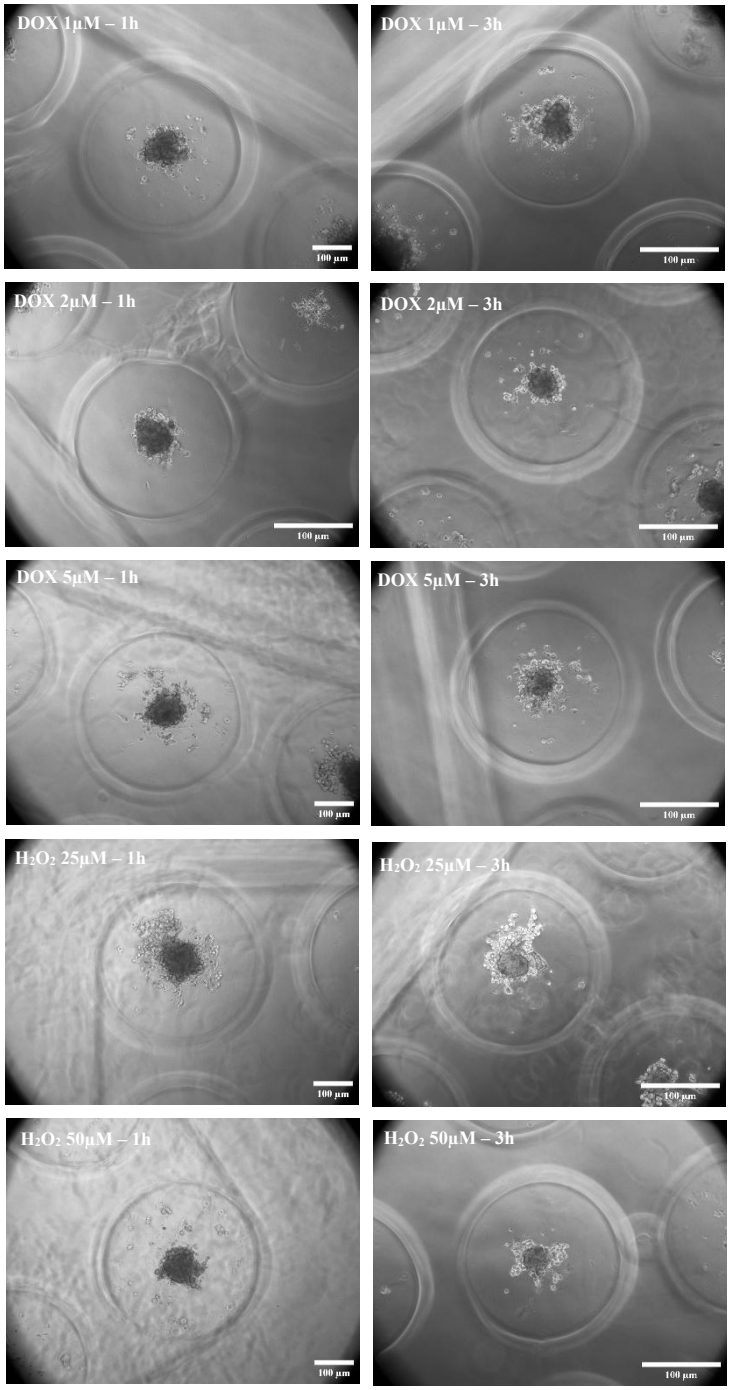

Figure 6.9 – MDA-MB-231 spheroids morphology after 1h and 3h of exposure to each treatment condition. Microscopy images obtained through 10x ampliation, scale: 100µm.

6.1.4. Comparison between Cell Lines

For further evaluation between the three cell line spheroids, the following variables were also analysed: solidity, eccentricity, compactness and maximum and minimum Feret diameters. Concerning these parameters: compactness values closer to 1 correspond to more regular and circular spheroids, whereas values further from 1 reflect less

compactness and higher irregularity; eccentricity ranges from 0 to 1 and describes de deviation from a perfect circle (value=0) to a highly elongated/elliptical shape (value=1); solidity also ranges from 0 to 1, with values closer to 1 symbolising more solid spheroids, without internal gaps or cavities. Besides those, the maximum and minimum Feret diameters were also measured; the maximum Feret diameter relates to longest distance between any two points along the spheroid external membrane and the minimum Feret diameter is the exact contrary, corresponding to the shortest span across the spheroid. Together, these measurements offer insight into spheroid size, elongation and overall shape, complementing the other evaluated morphological parameters.

Recurring to Figures 6.10 and 6.11, is it possible to observe a pattern that clearly distinguishes the larger size of MCF-7 spheroids, given the notable difference from MCF-10A and MDA-MB-231 spheroids, both in area and maximum and minimum Feret diameters – although if the spheroids from Figure 6.7 had been used on the morphological analysis, their size would be intermediary between MCF-7 and MCF-10A spheroids. This size difference is consistent across treatments and timepoints, indicating the naturally greater proliferative potential of this luminal BC line.

In contrast, MCF-10A and MDA-MB-231 spheroids display similar absolute dimensions, clustering together at the lower end of the size range. Despite their distinct biological nature – MCF-10A being a non-tumorigenic cell line and MDA-MB-231 being highly invasive and aggressive – both cell lines formed relatively small spheroids with comparable Feret diameters. This may suggest that their limitations in 3D cell growth processes, whether due to controlled proliferation (MCF-10A) or the loose cell-cell adhesion, typical of MDA-MB-231 spheroids, converge on a similar scale.

However, there are subtle variations that differ their response to the applied treatments. MDA-MB-231 spheroids exhibited greater variability over time, with momentary enlargements or reductions depending on drug and concentration, reflecting their well know capacity for rapid stress adaptation. As for MCF-10A spheroids, these remained more stable and compact, showing less significant changes.

Analysis of compactness, eccentricity and solidity revealed consistent and cell-line specific morphological patterns. Through Table 6.1 is possible to observe that MCF-7 spheroids exhibited the highest compactness values – with a mean ~2 at 1h, and ~1.97 at 3h –, indicating a more irregular perimeter, despite their size. MCF-10A showed the

lowest compactness (means ~1.34 and ~1.28), consistent with their highly circular geometry, while MDA-MB-231 is in-between those two cell lines, with means ~1.36 and ~1.43, but with greater dispersion, signalling apparent shape variability.

Eccentricity, which is presented on Table 6.2, shows that MCF-7 spheroids are moderately elongated, with mean values rising slightly from ~0.46 at 1h and ~0.50 at 3h. Notably, DOX 2µm produced a significant elongation at 3h (0.70), what suggests that larger MCF-7 aggregates are prone to subtle shape distortions under stress. MCF-10A spheroids maintained the lowest eccentricity overall, with mean values of 0.45 at 1h and 0.39 at 3h, apparently remaining consistently round ever under oxidative treatments. The highest variability was displayed by MDA-MB-231 spheroids, with an average of 0.50 at both timepoints, but varying from a value of 0.31 for DOX 1µM at 1h to a higher value of 0.62 for DOX 5µM at 3h, reflecting their dynamic cytoskeletal organization.

Table 6.3 represents the solidity results, which remained high across all lines but with subtle differences: MCF-10A showed the highest values – 0.97 and 0.98 –, confirming their dense, no cavity's structure. MCF-7 had slightly lower solidity (0.89 and 0.91) and MDA-MB-231 presented intermediate values (0.91-0.93), suggesting that even with irregular outlines, internal cohesion might still be preserved.

In sum, MCF-7 are clearly larger and prone to mild elongation while MCF-10A spheroids are smaller, round and tightly cohesive, with a size similar to MDA-MB-231 spheroids, that seem to be capable of reorganize their shape between more circular and elongated forms, depending on treatment.

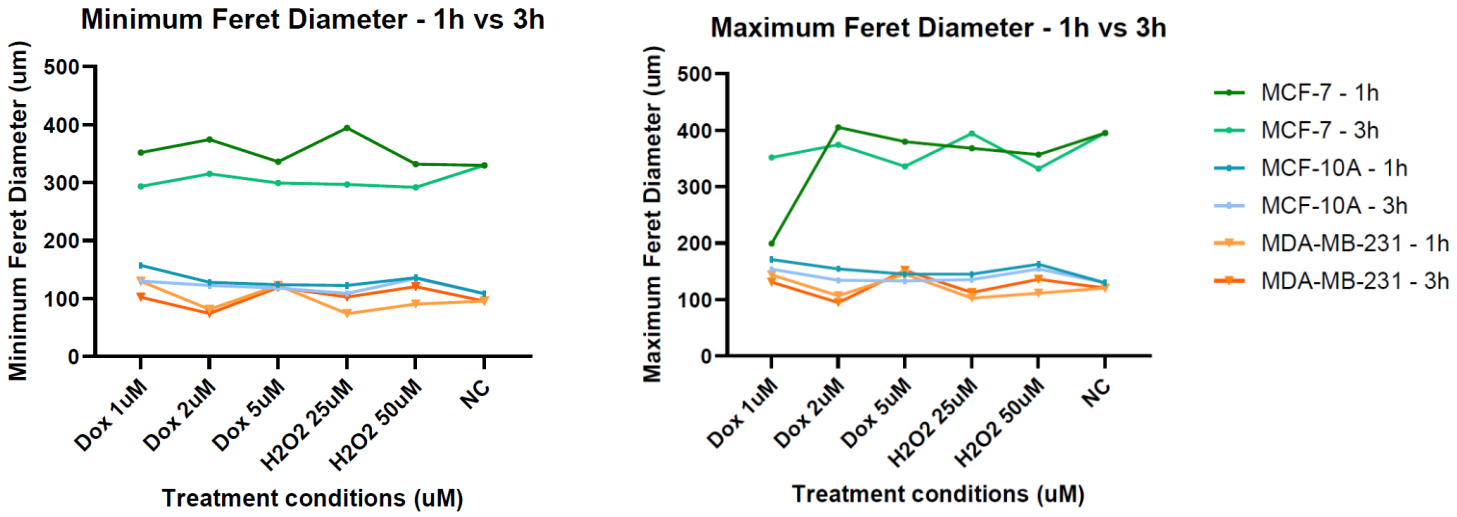

Figure 6.10 – Comparison of minimum and maximum Feret diameters at 1h and 3h for each treatment condition and cell line.

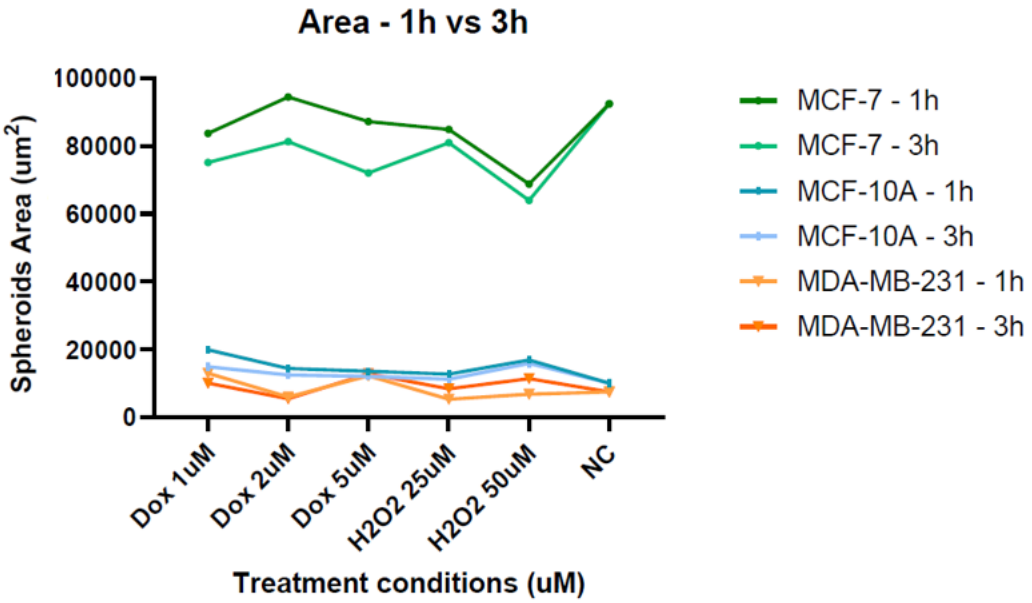

Figure 6.11 - Comparison of spheroids area at 1h and 3h for each treatment condition and cell line.

Table 6.1 - Compactness values for each cell line at 1h and 3h timepoints, with respective mean and standard deviation values.

Compactness	MCF-7		MCF-10A		MDA-MB-231	
	1h	3h	1h	3h	1h	3h
Dox 1uM	2.56	1.82	1.3	1.32	1.45	1.49
Dox 2uM	2.12	1.99	1.37	1.3	1.49	1.28
Dox 5uM	2.06	1.76	1.32	1.27	1.46	1.58
H2O2 25uM	1.72	2.19	1.29	1.25	0.66	1.36
H2O2 50uM	1.79	2.07	1.36	1.24	1.56	1.42
NC	1.93	-	1.38	-	1.54	-
Mean	2.03	1.97	1.34	1.28	1.36	1.43
SD	0.275	0.158	0.035	0.030	0.316	0.103

Table 6.2 - Eccentricity values for each cell line at 1h and 3h timepoints, with respective mean and standard deviation values.

Eccentricity	MCF-7		MCF-10A		MDA-MB-231	
	1h	3h	1h	3h	1h	3h
Dox 1uM	0.55	0.52	0.33	0.44	0.31	0.56
Dox 2uM	0.44	0.7	0.55	0.24	0.64	0.59
Dox 5uM	0.5	0.43	0.49	0.42	0.47	0.62
H2O2 25uM	0.34	0.62	0.45	0.48	0.65	0.31
H2O2 50uM	0.49	0.22	0.52	0.37	0.46	0.41
NC	0.45	-	0.37	-	0.47	-
Mean	0.46	0.50	0.45	0.39	0.50	0.50
SD	0.065	0.166	0.079	0.083	0.117	0.119

Table 6.3 - Solidity values for each cell line at 1h and 3h timepoints, with respective mean and standard deviation values.

Solidity	MCF-7		MCF-10A		MDA-MB-231	
	1h	3h	1h	3h	1h	3h
Dox 1uM	0.83	0.91	0.97	0.98	0.92	0.93
Dox 2uM	0.88	0.91	0.96	0.97	0.92	0.97
Dox 5uM	0.93	0.93	0.97	0.97	0.92	0.9
H2O2 25uM	0.91	0.89	0.98	0.98	0.9	0.94
H2O2 50uM	0.9	0.89	0.97	0.98	0.89	0.93
NC	0.9	-	0.96	-	0.91	-
Mean	0.89	0.91	0.97	0.98	0.91	0.93
SD	0.031	0.015	0.007	0.005	0.012	0.022

6.2. Analysis of DNA Damage

The comet assay was used to evaluate DNA damage in the spheroids derived from the three previously mentioned cell lines. As the fluorescence images obtained for comet scoring share a highly similar morphology across replicates and conditions, only representative examples are presented here, on Figure 6.12 to illustrate the appearance of comets.

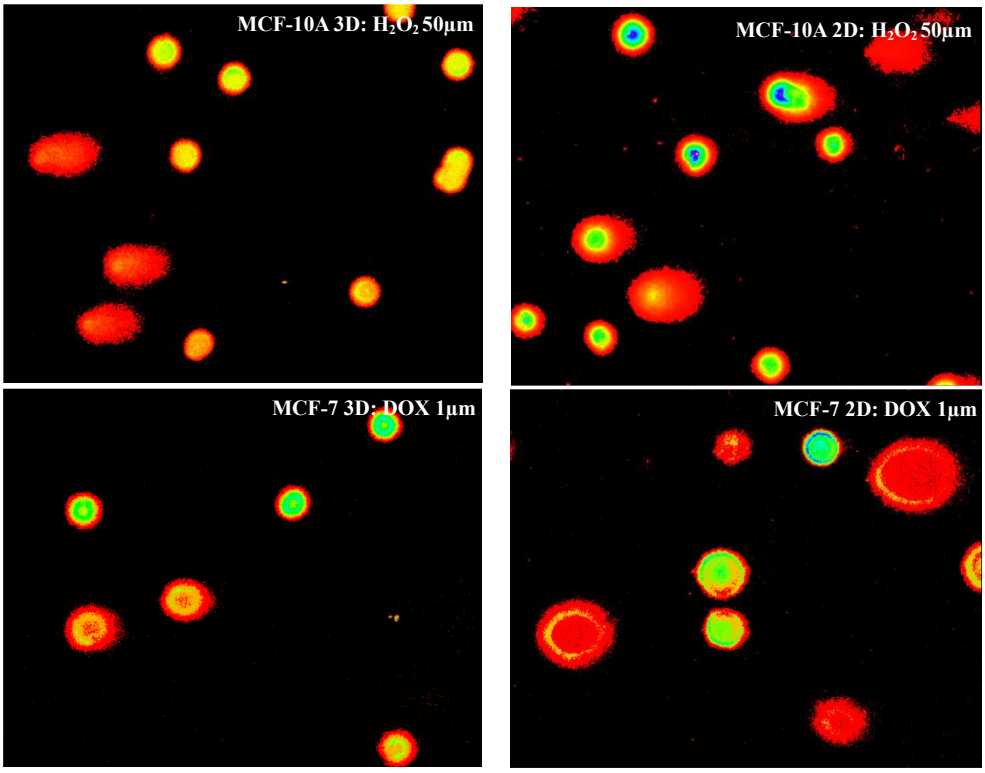

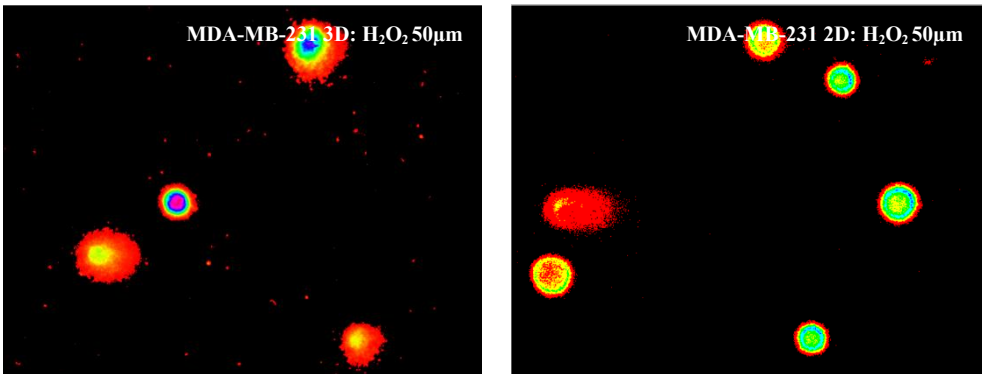

Figure 6.12 – Illustrative examples of microscopy images obtained from the ZEISS Z2 Microscope, with posterior analysis on the Comet Score software, after 3h exposure of certain treatments. Ampliation: 20x.

The following image (Figure 6.13) corresponds to an example of MCF-7 after 3h exposure to H_2O_2 25µm and is supposed to illustrate apparent cell apoptosis, which occurred mostly on MCF-7 spheroid prevenient cells, at both hydrogen peroxide concentrations.

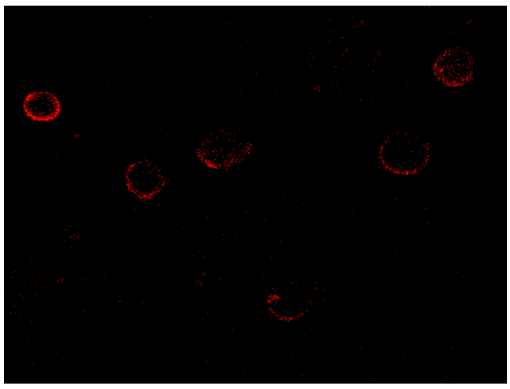

Figure 6.13 - Illustrative example of apoptotic cells on a microscopy image obtained from the ZEISS Z2 Microscope, with posterior analysis on the Comet Score software, after 3h exposure of H_2O_2 25µm. Ampliation: 20x.

6.2.1. MCF-10A

Both 2D and 3D MCF-10A cultures exhibited consistently low percentages of DNA in the comet tail under all experiment conditions, with mean values generally remaining under 20%. Thus, the increase in DNA damage was minimal and remained close to the NC levels, as seen in Figure 6.14.

The differences between 2D and 3D cultures suggest that even though spheroid organization may alter the genotoxic response of MCF-10A cells, it does not show a massive difference, likely because these cells already possess strong internal defenses against oxidative stress and effective DNA-repair mechanisms. Yet, it is possible to

observe that 2D cultures were more damaged with the DOX treatment than spheroids, which goes in line with previous studies (Lovitt et al., 2018).

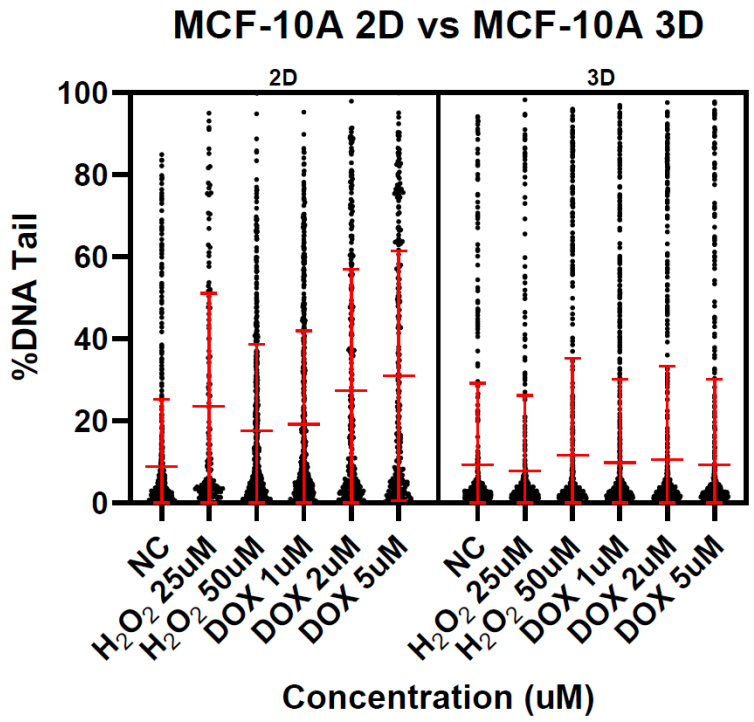

Figure 6.14 – Comet Assay results: DNA Damage in MCF-10A cell line. Comparison between 2D and 3D culture, for each treatment condition. The red lines represent the mean (longer bars) and the standard deviation (smaller bars).

6.2.2. MCF-7

In 2D culture, MCF-7 cells displayed a significant increase in DNA Tail % after exposure (Figure 6.15) to, particularly, H_2O_2 50µM (with a mean between 40% and 50%) and DOX 5µM (almost at 60%); in general, treatments based on DOX resulted in high DNA Tail percentages (both between 40% and 60%). By contrast, spheroids derived from this cell line showed a meaningful reduction on DOX treatments, however mean values were still between around 30% and 50%. It has been shown that DOX treatments present lower effectiveness when applied on 3D cultured MCF-7 cells, when compared to 2D culture (Lovitt et al., 2018).

As for H_2O_2, both concentrations resulted in similar mean values, showing a percentage of almost 60% of DNA damage on the comet tails; on Figure 6.13 is also possible to observe another possible reason for this increase, given that there was a high percentage of apparently apoptotic cells (some of which the program was not able to analyse even) on these two treatments. H_2O_2 is known for its capacity to cause cell death, where both

concentration and exposure highly affect the type of cell death – apoptosis, autophagy or necrosis(Ali et al., 2024; Chidawanyika & Supattapone, 2021).

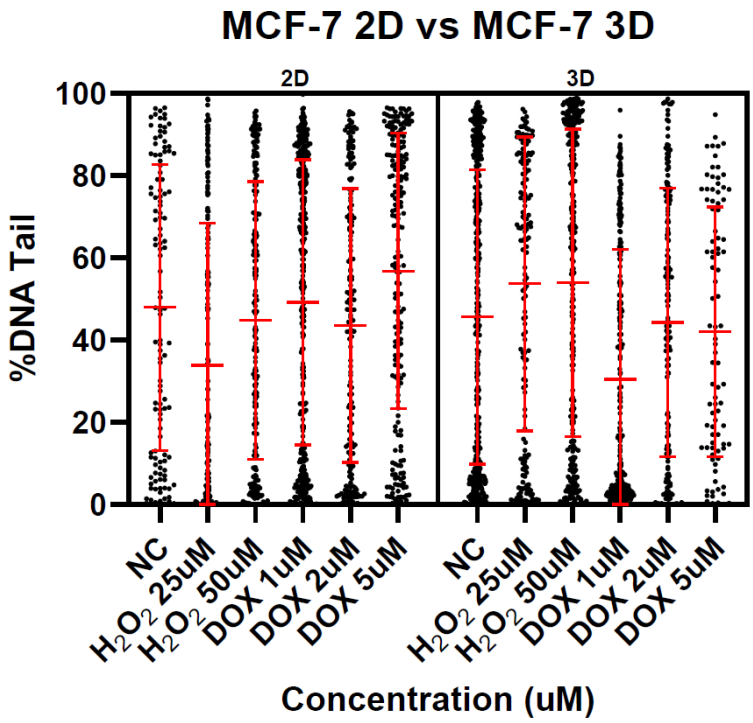

Figure 6.15 - Comet Assay results: DNA Damage in MCF-7 cell line. Comparison between 2D and 3D culture, for each treatment condition. The red lines represent the mean (longer bars) and the standard deviation (smaller bars).

6.2.3. MDA-MB-231

Two-dimension culture of MDA-MB-231 exhibited high DNA damage, as observed in Figure 6.16, with tail percentages often exceeding a mean of 40%, which aligns with their high proliferative rate and intrinsic genomic instability.

In 3D spheroids, DNA damage is significantly reduced across all treatments, with a more pronounced decrease than in MCF-7 spheroids. This response is likely due to some factors, such as formation of a necrotic core that limits diffusion of genotoxic agents and possible metabolic adaptation, that reduces ROS production in hypoxic inner cells. This behaviour goes in line with the clinical chemoresistance and aggressiveness of TNBC tumours, as well as with the fact that it has been previously discovered that BC spheroids are more resistant to chemotherapeutic drugs (Ali et al., 2024; Chavez et al., 2010; Dong et al., 2025).

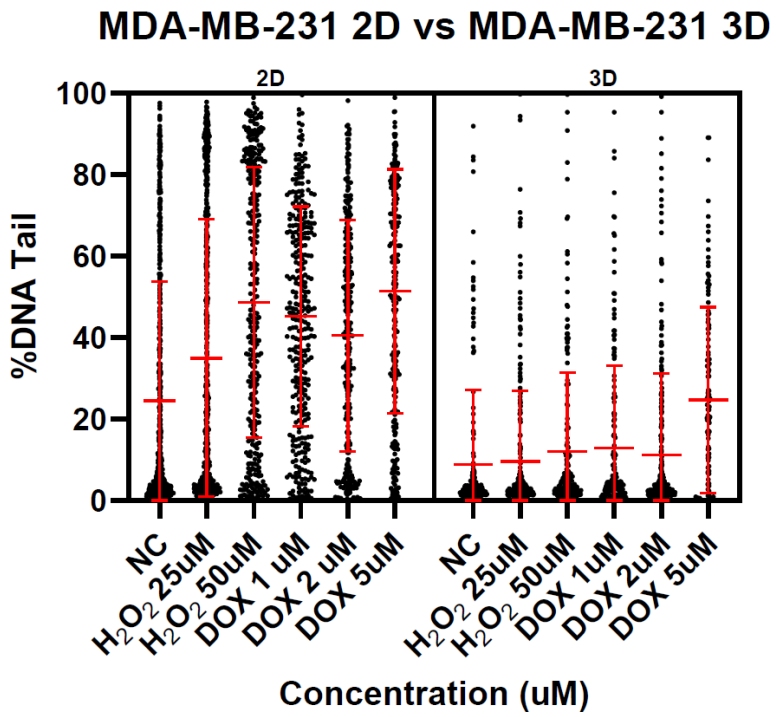

Figure 6.16 – Comet Assay results: DNA Damage in MDA-MB-231 cell line. Comparison between 2D and 3D culture, for each treatment condition. The red lines represent the mean (longer bars) and the standard deviation (smaller bars).

6.2.4. Overall Analysis of DNA Damage on BC spheroids

Hydrogen peroxide response to treatment from the three used cell lines is presented in Figure 6.17, where is possible to observe that the magnitude of this response is highly dependent on the cell line on which it was applied.

In MCF-10A spheroids, both concentrations induced low to moderate DNA damage, with only a slight increase at the higher concentration (50µM). This proposes that MCF-10A cells possess relatively effective antioxidant defense systems capable of easing oxidative stress at these concentrations. On the other hand, MCF-7 3D cultured cells displayed high levels of DNA damage even at the lower dose of H_2O_2, with a wide distribution of values and a considerable number of cells exceeding 80% DNA in the comet tails. Nevertheless, the mean values suggest that most cells displayed values within the 40-60% range. These results highlight the susceptibility of MCF-7 cells to H_2O_2 and imply oxidative stress as a significant contributor to genomic instability in luminal BC, which is in line with the main role of H_2O_2 – if increased beyond homeostatic concentrations, leads to oxidative stress and if not alleviated through antioxidant responses, consequences like cell death can occur. For MDA-MB-231 spheroids, DNA damage levels were moderate and

relatively consistent across both H_2O_2 concentrations, suggesting an enhanced capacity to neutralize oxidative stress. This is consistent with previous reports that TNBC cell upregulate antioxidant enzymes and exhibit increased redox adaptability, which may contribute to their survival under oxidative and therapeutic stress (Ali et al., 2024; Chidawanyika & Supattapone, 2021).

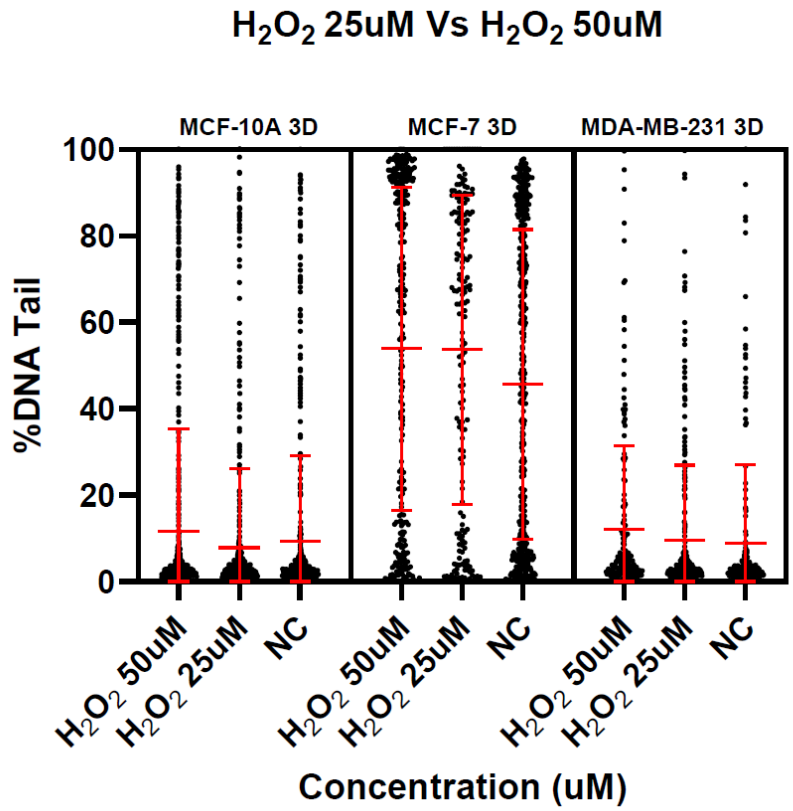

Figure 6.17 – Comet Assay results: Comparison between H_2O_2 25µM, H_2O_2 50µM and Negative Control (NC), for each cell line spheroids. The red lines represent the mean (longer bars) and the standard deviation (smaller bars).

As shown in Figure 6.18, DOX treatment induced varying degrees of DNA damage across the three cell lines. In MCF-10A spheroids, exposure to DOX 1µM and DOX 5µM, resulted in relatively low levels of DNA damage. In contrast, MCF-7 spheroids exhibited a pronounced and dose-dependent increase in DNA damage, where the %DNA in comet tails was highly elevated at DOX 5µM, when compared to DOX 1µM, which may be indicative of a heightened sensitivity to the drug. This aligns with the known susceptibility of luminal BC cells to inhibitors like DOX, possibly due to their higher proliferation rate and reduced DNA repair capacity. As for MDA-MB-231 spheroids, these showed moderate levels of DNA damage, with slight differences between the two concentrations. This may reflect intrinsic resistance mechanisms, often found in TNBC, such as enhanced DNA repair pathways and resistance to apoptosis. Plus, the relatively

broad distribution of %DNA tail values within this cell line further highlights cellular heterogeneity, which is commonly observed in aggressive TNBC phenotype, like MDA-MB-231 (Lovitt et al., 2018; Ncube et al., 2023)

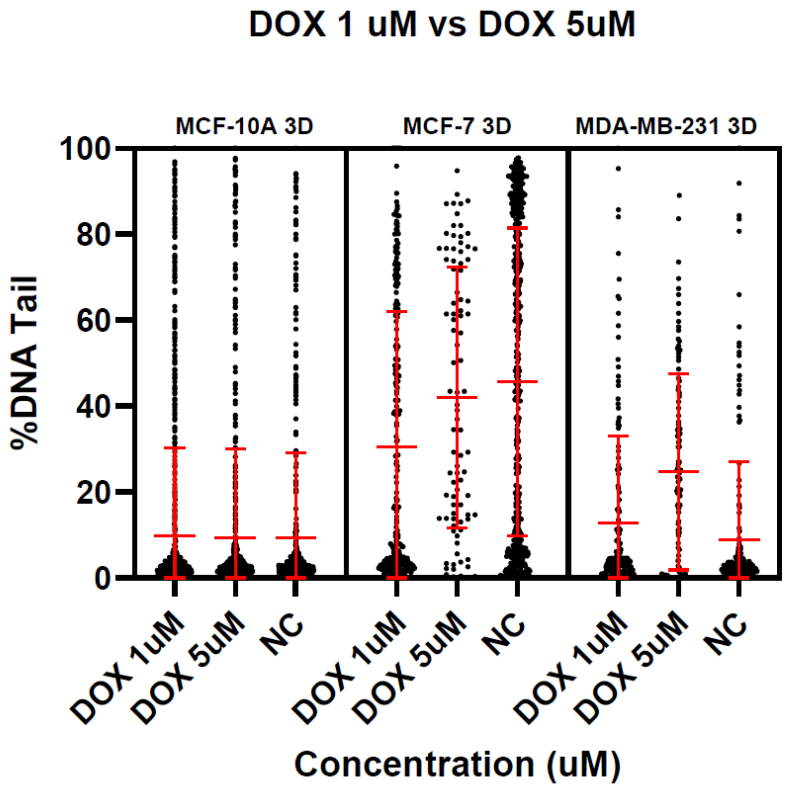

Figure 6.18 – Comet Assay results: Comparison between Dox 1µM, Dox 5µM and NC, for each cell lines spheroids. The red lines represent the mean (longer bars) and the standard deviation (smaller bars).

6.3. Linking Spheroids Morphology, Drug Resistance and DNA Damage

Regarding spheroids morphology, it was evident that MCF-10A formed smaller, more regular and highly compact and circular spheroids, presenting high solidity even after treatments. MCF-7 originated larger spheroids, with higher loss of centre cohesion and greater morphological variability, given perimeter irregularities, seen with the Feret diameters. In contrast, MDA-MB-231 produced less cohesive and more irregular spheroids, susceptible to rapid variations on size depending on the applied treatment.

The comet assay exposed relevant differences between 2D and 3D cultures, with the latter showing higher resistance to damage, reinforcing the functional relevance of tri-

dimensional models for chemotherapeutic agent's studies in BC. Dox treatments presented a dose-dependent effect, causing significant DNA fragmentation particularly in MCF-7 and MDA-MB-231 cultures, while MCF-10A was, apparently, less affected – which can be a sign of its effective repair systems. Hydrogen peroxide responses were also cell line dependent, with MCF-7 showing increased susceptibility and a higher appearance of apoptotic cells.

Spheroids with higher compactness and regularity, like MCF-10A spheroids present increased cell-cell contact, strong cohesion and homogeneous distribution of nutrients, whereas irregular spheroids like MCF-7 and MDA-MB-231 show functional heterogeneity and necrotic zones. This data supports that both compactness and solidity are connected to drug resistance. Three-dimensional structures generate oxygen, nutrient and drug gradients that consequently create different responses from each cell line and respective treatments. In larger and less compact spheroids, central cells may become hypoxic and quiescent, therefore less sensitive to induced genetic damage, as the proliferation rate is lower and the capacity to activate antioxidant and repairing systems higher. On the other hand, less cohesive 3D structures allow for higher contact with external agents, becoming more susceptible to oxidative stress and apoptosis, particularly in the peripheric zone(Pinto et al., 2020).

The tumours molecular subtype also affects its morphology and damage response. Luminal subtypes, like MCF-7, tend to form larger, less solid spheroids with higher sensitivity to drugs, which act on peripheric cells, as was shown in this work. TNBC, like MDA-MB-231, tend to form irregular structures, with increased morphological plasticity and rapid adaptation to induced stress, reflecting their effective DDR mechanisms. This morphological heterogeneity seems to be directly related to the obtained responses in the comet assays, where was seen that MCF-10A spheroids – more compact – presented lower DNA fragmentation levels, suggesting vigorous repair systems and reduced drug penetration. MCF-7 irregular structures allow chemotherapeutic agents to harm peripherical cells, increasing the DNA damage on the comet tails e apoptosis occurrence. MDA-MB-231 spheroids, although irregular, can quickly reorganize their structure and activate repair systems (Imamura et al., 2014).

7. Conclusion

This work consisted of a broad analysis of the effect of chemotherapeutic drugs on three distinct BC cell lines, both in 2D and 3D culture. The integration of 2D and 3D culture, treatment with DOX and H_2O_2, the comet assay and the morphological analysis were all processes that contributed to a deeper understanding of the relation between spheroids morphology, drug resistance and response to treatment, aiming to shape the final results into a compact understanding of how spheroids cellular architecture influences chemotherapeutic sensitivity and DNA damage response in BC models. This approach provides a background for correlating spheroid morphology with treatment outcomes, potentially guiding more effective therapeutic strategies and highlighting the importance of 3D culture systems in preclinical drug testing.

Collectively, these outcomes demonstrate that spheroid compactness and solidity are key elements of drug response, influencing nutrient and oxygen gradients, drug diffusion and DNA damage repair. Compact 3D spheroids limit chemotherapeutic access and promote resistance, whereas irregular spheroids allow greater drug penetration but exhibit heterogeneous functional responses. This resistance is further reinforced by the spatial heterogeneity within spheroids, where quiescent cells in the core are inherently less sensitive to treatment, and the dense, ECM-rich layer impedes the penetration of chemotherapy. Consequently, spatial organization not only shapes cellular phenotypes but also contributes to differential therapeutic responses. The differences observed between 2D, and 3D cultures accentuate the physiological relevance of 3D models, which more accurately mimic tumour microenvironments and reveal resistance mechanisms not captured in traditional 2D systems (Ncube et al., 2025).

By linking morphology, DNA damage response and chemotherapeutic sensitivity, this study reinforces the value of 3D cultured models as predictive tools in BC research and provides insights that may guide the development of personalized therapeutic approaches informed by tumour architecture and molecular subtype. In addition to demonstrating the structural influence of spheroid compactness and heterogeneity on treatment results, these findings highlight the dynamic interaction between the tumour microenvironment and cellular repair mechanisms as a critical determining factor of therapeutic success. The observed cell line specific differences accentuate that BC is not a uniform disease but a

complex selection of molecular subtypes whose growth patterns and adaptive capacities directly impact drug penetration and genetic stability.

Nevertheless, some limitations should be acknowledged. Variability in spheroid size and morphology (particularly in MDA-MB-231) likely occurs due to both intrinsic biological properties and minor procedure variations, highlighting the challenges of standardization in 3D culture systems. Besides, quantification in the comet assay remains partially dependent on software parameters and sample variability, while limited diffusion of genotoxic agents and occasional cell loss during processes, particularly during the comet assay procedure, may also affect outcomes. On that thought, in order to optimize the obtained results from the first 3D experiments, the comet assay protocol was slightly changed to minimize cell loss and reduce the risk of obtaining highly inconsistent results across samples. This adjustment helped ensure that the DNA damage measurements reflected the true cellular response more accurately, increasing the reliability of the obtained 3D results. Additionally, fluctuations in cell quantities per sample can influence comparability and should be considered when interpreting the results.

Overall, this study confirms that 3D models are indispensable tools for BC investigation, offering a more physiologically relevant platform for understanding tumour biology, treatment response and chemoresistance. Incorporating structural and functional parameters into preclinical testing may therefore improve the accuracy of drug screening, reduce possible gaps between *in vitro* and *in vivo* responses and guide the development of more personalized and effective treatment protocols. Future studies should focus on optimizing culture protocols and automated quantification, expanding analyses to additional genotoxic agents, possibly integrating gene and protein expression studies related to DNA repair and resistance.

In conclusion, the result of this work demonstrates the power of 3D spheroid models to more accurately predict drug responses, providing a solid basis for the development of more effective and individualized BC treatments.

8. References

About breast cancer staging and grades. (2023, May 16). Cancer Research UK.

Ali, T., Li, D., Ponnamperumage, T. N. F., Peterson, A. K., Pandey, J., Fatima, K., Brzezinski, J., Jakusz, J. A. R., Gao, H., Koelsch, G. E., Murugan, D. S., & Peng, X. (2024). Generation of Hydrogen Peroxide in Cancer Cells: Advancing Therapeutic Approaches for Cancer Treatment. In Cancers (Vol. 16, Issue 12). Multidisciplinary Digital Publishing Institute (MDPI). https://doi.org/10.3390/cancers16122171

Al-malky, H. S., Al Harthi, S. E., & Osman, A. M. M. (2020). Major obstacles to doxorubicin therapy: Cardiotoxicity and drug resistance. In Journal of Oncology Pharmacy Practice (Vol. 26, Issue 2, pp. 434–444). SAGE Publications Ltd. https://doi.org/10.1177/1078155219877931

Anampa, J., Makower, D., & Sparano, J. A. (2015). Progress in adjuvant chemotherapy for breast cancer: An overview. In BMC Medicine (Vol. 13, Issue 1). BioMed Central Ltd. https://doi.org/10.1186/s12916-015-0439-8

Bhushan, A., Gonsalves, A., & Menon, J. U. (2021). Current state of breast cancer diagnosis, treatment, and theranostics. In Pharmaceutics (Vol. 13, Issue 5). MDPI. https://doi.org/10.3390/pharmaceutics13050723

Breslin, S., & O'driscoll, L. (2016). The relevance of using 3D cell cultures, in addition to 2D monolayer cultures, when evaluating breast cancer drug sensitivity and resistance. In Oncotarget (Vol. 7, Issue 29). www.impactjournals.com/oncotarget/

Brown T. A. (2007). Genomes 3 (3rd Edition). Garland Science Pub.

Cailleau,', R., Olive, M., & Cruciger, Q. V. J. (1978). LONG-TERM HUMAN BREAST CARCINOMA CELL LINES OF METASTATIC ORIGIN: PRELIMINARY CHARACTERIZATION. In IN VITRO (Vol. 14, Issue 11).

Carusillo, A., & Mussolino, C. (2020). DNA Damage: From Threat to Treatment. In Cells (Vol. 9, Issue 7). NLM (Medline). https://doi.org/10.3390/cells9071665

Casting, Equilibrating and Seeding the 3D Petri Dish. (n.d.). Https://Www.Microtissues.Com/Protocols.

Chatterjee, N., & Walker, G. C. (2017). Mechanisms of DNA damage, repair, and mutagenesis. In Environmental and Molecular Mutagenesis (Vol. 58, Issue 5, pp. 235–263). John Wiley and Sons Inc. https://doi.org/10.1002/em.22087

Chavez, K. J., Garimella, S. V., & Lipkowitz, S. (2010). Triple negative breast cancer cell lines: One tool in the search for better treatment of triple negative breast cancer. Breast Disease, 32(1–2), 35–48. https://doi.org/10.3233/BD-2010-0307

Chidawanyika, T., & Supattapone, S. (2021). Hydrogen Peroxide-induced Cell Death in Mammalian Cells. Journal of Cellular Signaling, 2(3). https://doi.org/10.33696/signaling.2.052

Collins, A., Møller, P., Gajski, G., Vodenková, S., Abdulwahed, A., Anderson, D., Bankoglu, E. E., Bonassi, S., Boutet-Robinet, E., Brunborg, G., Chao, C., Cooke, M. S., Costa, C., Costa, S., Dhawan, A., de Lapuente, J., Bo', C. Del, Dubus, J., Dusinska, M., … Azqueta, A. (2023). Measuring DNA modifications with the comet assay: a compendium of protocols. In Nature Protocols (Vol. 18, Issue 3, pp. 929–989). Springer Nature. https://doi.org/10.1038/s41596-022-00754-y

COMȘA, Ș., CÎMPEAN, A. M., & RAICA, M. (2015). The Story of MCF-7 Breast Cancer Cell Line: 40 years of Experience in Research. Anticancer Research.

Dai, X., Cheng, H., Bai, Z., & Li, J. (2017). Breast cancer cell line classification and Its relevance with breast tumor subtyping. In Journal of Cancer (Vol. 8, Issue 16, pp. 3131–3141). Ivyspring International Publisher. https://doi.org/10.7150/jca.18457

Dhawan, A., Bajpayee, M., & Parmar, D. (2009). Comet assay: A reliable tool for the assessment of DNA damage in different models. In Cell Biology and Toxicology (Vol. 25, Issue 1, pp. 5–32). https://doi.org/10.1007/s10565-008-9072-z

Dong, R., Wang, J., Guan, R., Sun, J., Jin, P., & Shen, J. (2025). Role of Oxidative Stress in the Occurrence, Development, and Treatment of Breast Cancer. In Antioxidants (Vol. 14, Issue 1). Multidisciplinary Digital Publishing Institute (MDPI). https://doi.org/10.3390/antiox14010104

Duval, K., Grover, H., Han, L. H., Mou, Y., Pegoraro, A. F., Fredberg, J., & Chen, Z. (2017). Modeling physiological events in 2D vs. 3D cell culture. In Physiology (Vol. 32, Issue 4, pp. 266–277). American Physiological Society. https://doi.org/10.1152/physiol.00036.2016

Faraji, A., Manshadi, H. R. D., Mobaraki, M., Zare, M., & Houshmand, M. (2016). Association of ABCB1 and SLC22A16 gene polymorphisms with incidence of doxorubicin-induced febrile neutropenia: A survey of iranian breast cancer patients. In PLoS ONE (Vol. 11, Issue 12). Public Library of Science. https://doi.org/10.1371/journal.pone.0168519

Fisher, M. F., & Rao, S. S. (2020). Three-dimensional culture models to study drug resistance in breast cancer. In Biotechnology and Bioengineering (Vol. 117, Issue 7, pp. 2262–2278). John Wiley and Sons Inc. https://doi.org/10.1002/bit.27356

Fontoura, J. C., Viezzer, C., dos Santos, F. G., Ligabue, R. A., Weinlich, R., Puga, R. D., Antonow, D., Severino, P., & Bonorino, C. (2020). Comparison of 2D and 3D cell culture models for cell growth, gene expression and drug resistance. Materials Science and Engineering C, 107. https://doi.org/10.1016/j.msec.2019.110264

Garnique, A. del M. B., Parducci, N. S., de Miranda, L. B. L., de Almeida, B. O., Sanches, L., & Machado-Neto, J. A. (2024). Two-Dimensional and Spheroid-Based Three-Dimensional Cell Culture Systems: Implications for Drug Discovery in Cancer. Drugs and Drug Candidates, 3(2), 391–409. https://doi.org/10.3390/ddc3020024

Glei, M., Schneider, T., & Schlörmann, W. (2016). Comet assay: an essential tool in toxicological research. In Archives of Toxicology (Vol. 90, Issue 10, pp. 2315–2336). Springer Verlag. https://doi.org/10.1007/s00204-016-1767-y

Hakem, R. (2008). DNA-damage repair; the good, the bad, and the ugly. EMBO Journal, 27(4), 589–605. https://doi.org/10.1038/emboj.2008.15

Harvesting Multi-cellular Microtissues from the 3D Petri Dish. (n.d.). Https://Www.Microtissues.Com/Protocols.

Hassan, M. S. U., Ansari, J., Spooner, D., & Hussain, S. A. (2010). Chemotherapy for breast cancer (review). In Oncology Reports (Vol. 24, Issue 5, pp. 1121–1131). Spandidos Publications. https://doi.org/10.3892/or_00000963

Hong, R., & Xu, B. (2022). Breast cancer: an up-to-date review and future perspectives. In Cancer Communications (Vol. 42, Issue 10, pp. 913–936). John Wiley and Sons Inc. https://doi.org/10.1002/cac2.12358

Huang, Z., Yu, P., & Tang, J. (2020). Characterization of triple-negative breast cancer MDA-MB-231 cell spheroid model. OncoTargets and Therapy, 13, 5395–5405. https://doi.org/10.2147/OTT.S249756

Imamura, Y., Mukohara, T., Shimono, Y., Funakoshi, Y., Chayahara, N., Toyoda, M., Kiyota, N., Takao, S., Kono, S., Nakatsura, T., & Minami, H. (2015). Comparison of 2D- and 3D-culture models as drug-testing platforms in breast cancer. Oncology Reports, 33(4), 1837–1843. https://doi.org/10.3892/or.2015.3767

Imbalzano, K. M., Tatarkova, I., Imbalzano, A. N., & Nickerson, J. A. (2009). Increasingly transformed MCF-10A cells have a progressively tumor-like phenotype in three-dimensional basement membrane culture. Cancer Cell International, 9. https://doi.org/10.1186/1475-2867-9-7

Jensen, C., & Teng, Y. (2020). Is It Time to Start Transitioning From 2D to 3D Cell Culture? In Frontiers in Molecular Biosciences (Vol. 7). Frontiers Media S.A. https://doi.org/10.3389/fmolb.2020.00033

Kang, T. H. (2023). DNA Damage, Repair, and Cancer Metabolism. In International Journal of Molecular Sciences (Vol. 24, Issue 22). Multidisciplinary Digital Publishing Institute (MDPI). https://doi.org/10.3390/ijms242216430

Kapałczyńska, M., Kolenda, T., Przybyła, W., Zajączkowska, M., Teresiak, A., Filas, V., Ibbs, M., Bliźniak, R., Łuczewski, Ł., & Lamperska, K. (2018). 2D and 3D cell cultures – a comparison of different types of cancer cell cultures. Archives of Medical Science, 14(4), 910–919. https://doi.org/10.5114/aoms.2016.63743

Kenny, P. A., Lee, G. Y., Myers, C. A., Neve, R. M., Semeiks, J. R., Spellman, P. T., Lorenz, K., Lee, E. H., Barcellos-Hoff, M. H., Petersen, O. W., Gray, J. W., & Bissell, M. J. (2007). The morphologies of breast cancer cell lines in three-

dimensional assays correlate with their profiles of gene expression. Molecular Oncology, 1(1), 84–96. https://doi.org/10.1016/j.molonc.2007.02.004

Li, L. Y., Guan, Y. Di, Chen, X. S., Yang, J. M., & Cheng, Y. (2021). DNA Repair Pathways in Cancer Therapy and Resistance. In Frontiers in Pharmacology (Vol. 11). Frontiers Media S.A. https://doi.org/10.3389/fphar.2020.629266

Liao, W., McNutt, M. A., & Zhu, W. G. (2009). The comet assay: A sensitive method for detecting DNA damage in individual cells. In Methods (Vol. 48, Issue 1, pp. 46–53). https://doi.org/10.1016/j.ymeth.2009.02.016

Liu, H., Zang, C., Fenner, M. H., Possinger, K., & Elstner, E. (2003). PPARγ γ γ ligands and ATRA inhibit the invasion of human breast cancer cells in vitro. In Breast Cancer Research and Treatment (Vol. 79).

Lovitt, C. J., Shelper, T. B., & Avery, V. M. (2015). Evaluation of chemotherapeutics in a three-dimensional breast cancer model. Journal of Cancer Research and Clinical Oncology, 141(5), 951–959. https://doi.org/10.1007/s00432-015-1950-1

Lovitt, C. J., Shelper, T. B., & Avery, V. M. (2018). Doxorubicin resistance in breast cancer cells is mediated by extracellular matrix proteins. BMC Cancer, 18(1). https://doi.org/10.1186/s12885-017-3953-6

Lu, Y., Liu, Y., & Yang, C. (2017). Evaluating in vitro DNA damage using comet assay. Journal of Visualized Experiments, 2017(128). https://doi.org/10.3791/56450

Møller, P. (2018). The comet assay: Ready for 30 more years. In Mutagenesis (Vol. 33, Issue 1, pp. 1–7). Oxford University Press. https://doi.org/10.1093/mutage/gex046

Ncube, K. N., Jurgens, T., Steenkamp, V., Cromarty, A. D., van den Bout, I., & Cordier, W. (2023). Comparative Evaluation of the Cytotoxicity of Doxorubicin in BT-20 Triple-Negative Breast Carcinoma Monolayer and Spheroid Cultures. Biomedicines, 11(5). https://doi.org/10.3390/biomedicines11051484

Ncube, K. N., van den Bout, I., Willers, C., Gouws, C., & Cordier, W. (2025). Utility of Multicellular Spheroids for Investigating Mechanisms of Chemoresistance in Triple-Negative Breast Cancer. In International Journal of Molecular

Sciences (Vol. 26, Issue 15). Multidisciplinary Digital Publishing Institute (MDPI). https://doi.org/10.3390/ijms26157503

Nicoletto, R. E., & Ofner, C. M. (2022). Cytotoxic mechanisms of doxorubicin at clinically relevant concentrations in breast cancer cells. In Cancer Chemotherapy and Pharmacology (Vol. 89, Issue 3, pp. 285–311). Springer Science and Business Media Deutschland GmbH. https://doi.org/10.1007/s00280-022-04400-y

Nunes, A. S., Barros, A. S., Costa, E. C., Moreira, A. F., & Correia, I. J. (2019). 3D tumor spheroids as in vitro models to mimic in vivo human solid tumors resistance to therapeutic drugs. In Biotechnology and Bioengineering (Vol. 116, Issue 1, pp. 206–226). John Wiley and Sons Inc. https://doi.org/10.1002/bit.26845

'Orrantia-Borunda, E., 'Anchondo-Nuñez, P., 'Acuña-Aguilar, L. E., 'Gómez-Valles, F. O. ', & 'Ramírez-Valdespino, C. A. (2022). Subtypes of Breast Cancer. Brisbane(AU): Exon Publications, 46–57.

Pharmaceu Sci, G. J., Sudhir Ambekar, S., Shrisel Hattur, S., & Budha Bule, P. (2017). DNA: Damage and Repair Mechanisms in Humans. In Review Article (Vol. 3).

Pinto, B., Henriques, A. C., Silva, P. M. A., & Bousbaa, H. (2020). Three-dimensional spheroids as in vitro preclinical models for cancer research. In Pharmaceutics (Vol. 12, Issue 12, pp. 1–38). MDPI AG. https://doi.org/10.3390/pharmaceutics12121186

Saji Joseph, J., Tebogo Malindisa, S., & Ntwasa, M. (2019). Two-Dimensional (2D) and Three-Dimensional (3D) Cell Culturing in Drug Discovery. In Cell Culture. IntechOpen. https://doi.org/10.5772/intechopen.81552

Sanju Tamang. (2023, September 8). DNA Damage and DNA Repair: Types and Mechanism. Microbe Notes.

Shah, C., Al-Hilli, Z., & Vicini, F. (2024). Advances in Breast Cancer Radiotherapy: Implications for Current and Future Practice. https://doi.org/10.1200/OP.21

Smolarz, B., Zadrożna Nowak, A., & Romanowicz, H. (2022). Breast Cancer—Epidemiology, Classification, Pathogenesis and Treatment (Review of

Literature). In Cancers (Vol. 14, Issue 10). MDPI. https://doi.org/10.3390/cancers14102569

Wilkinson, L., & Gathani, T. (2022). Understanding breast cancer as a global health concern. In British Journal of Radiology (Vol. 95, Issue 1130). British Institute of Radiology. https://doi.org/10.1259/BJR.20211033

Annexes

Tables

Table A.1 – Specifications for each comet assay solution

Chemical Element	Supplier	Molar Mass	Concentration	Measeaurements	Solutions
NaOH	Sigma-Aldrich	40g/mol	10M	500 ml ddH2O 200g NaOH	Electrophoresis Tampon
EDTA	Sigma-Aldrich	372,24g/mol	100mM	1l ddH2O 37,22g EDTA	Lysis Solution
			200mM	500ml ddH2O 37,22g EDTA	Electrophoresis Tampon
NaCl	Sigma-Aldrich	58,44g/mol	2,5M	1l ddH2O 146,1g NaOH	Lysis Solution
TrisBase	Fisher Bioreagents	121,14g/mol	10mM	1l ddH2O 1,21g TrisBase	Lysis Solution
			0,4M	1l ddH2O 48,45g TrisBase	Neutralization Tampon

Table A.2 - Extras and pH for each comet assay solution.

Solutions	Extras	pH
Electrophoresis Tampon	-	≥13
Lysis Solution	+1% Triton Detergent x-100	10
Neutralization Tampon	-	7,5